ARTICLE

doi:10.1038/nature12921

Fifty thousand years of Arctic vegetation and megafaunal diet

Eske Willerslev[1]*, John Davison[2]*, Mari Moora[2]*, Martin Zobel[2]*, Eric Coissac[3]*, Mary E. Edwards[4]*, Eline D. Lorenzen[1,5]*, Mette Vestergård[1]*, Galina Gussarova[6,7]*, James Haile[1,8]*, Joseph Craine[9], Ludovic Gielly[3], Sanne Boessenkool[6]†, Laura S. Epp[6]†, Peter B. Pearman[10], Rachid Cheddadi[11], David Murray[12], Kari Anne Bråthen[13], Nigel Yoccoz[13], Heather Binney[4], Corinne Cruaud[14], Patrick Wincker[14], Tomasz Goslar[15,16], Inger Greve Alsos[17], Eva Bellemain[6]†, Anne Krag Brysting[18], Reidar Elven[6], Jørn Henrik Sønstebø[6], Julian Murton[19], Andrei Sher[20]‡, Morten Rasmussen[1], Regin Rønn[21], Tobias Mourier[1], Alan Cooper[22], Jeremy Austin[22], Per Möller[23], Duane Froese[24], Grant Zazula[25], François Pompanon[3], Delphine Rioux[3], Vincent Niderkorn[26], Alexei Tikhonov[27], Grigoriy Savvinov[28], Richard G. Roberts[29], Ross D. E. MacPhee[30], M. Thomas P. Gilbert[1], Kurt H. Kjær[1], Ludovic Orlando[1], Christian Brochmann[6]* & Pierre Taberlet[3]*

Although it is generally agreed that the Arctic flora is among the youngest and least diverse on Earth, the processes that shaped it are poorly understood. Here we present 50 thousand years (kyr) of Arctic vegetation history, derived from the first large-scale ancient DNA metabarcoding study of circumpolar plant diversity. For this interval we also explore nematode diversity as a proxy for modelling vegetation cover and soil quality, and diets of herbivorous megafaunal mammals, many of which became extinct around 10 kyr BP (before present). For much of the period investigated, Arctic vegetation consisted of dry steppe–tundra dominated by forbs (non-graminoid herbaceous vascular plants). During the Last Glacial Maximum (25–15 kyr BP), diversity declined markedly, although forbs remained dominant. Much changed after 10 kyr BP, with the appearance of moist tundra dominated by woody plants and graminoids. Our analyses indicate that both graminoids and forbs would have featured in megafaunal diets. As such, our findings question the predominance of a Late Quaternary graminoid-dominated Arctic mammoth steppe.

It can be argued that Arctic vegetation during the proximal Quaternary (the last circa 50 kyr) is less well understood than the ecology and population dynamics of the mammals that consumed it, despite the overall uniformity and low floristic diversity of Arctic vegetation[1,2]. Analyses of vegetation changes during this interval have been based mainly on fossil pollen. Although highly informative, records tend to be biased towards high pollen producers such as many graminoids (grasses, sedges and rushes) and *Artemisia*, which can obscure the abundance of other forms such as many insect-pollinated forbs[1]. Arctic pollen records are rarely comprehensively identified to species level, which underestimates actual diversity[3]. These problems are to some extent ameliorated by plant macrofossil studies (for example, ref. 4), which may provide detailed records of local vegetation. However, macrofossil studies are far less common, have their own taxonomic constraints, and usually cannot provide quantitative estimates of abundance.

In recent years, a complementary approach has emerged that uses plant and animal ancient DNA preserved in permafrost sediments[5]. Such environmental DNA[6] does not derive primarily from pollen, bones or teeth, but likely from above- and below-ground plant biomass, faeces, discarded cells and urine preserved in sediments[7–9]. Like macrofossils, environmental DNA appears to be local in origin[6,10–12] and, in principle, the survival of a few fragmented DNA molecules is sufficient for retrieval and taxonomic identification[13].

Environmental DNA can supply the fraction of the plant community not readily identifiable by pollen analysis and, to some extent, macrofossils, particularly in vegetation dominated by non-woody growth forms[7].

[1]Centre for GeoGenetics, Natural History Museum, University of Copenhagen, Oster Voldgade 5-7, DK-1350 Copenhagen K, Denmark. [2]Department of Botany, Institute of Ecology and Earth Sciences, University of Tartu, 40 Lai Street, 51005 Tartu, Estonia. [3]Laboratoire d'Ecologie Alpine (LECA) CNRS UMR 5553, University Joseph Fourier, BP 53, 38041 Grenoble Cedex 9, France. [4]Geography and Environment, University of Southampton, Southampton SO17 1BJ, UK. [5]Department of Integrative Biology, University of California Berkeley, 1005 Valley Life Sciences Building, Berkeley, 94720 California, USA. [6]National Centre for Biosystematics, Natural History Museum, University of Oslo, PO Box 1172, Blindern, NO-0318 Oslo, Norway. [7]Department of Botany, Saint Petersburg State University, Universitetskaya nab. 7/9, 199034 Saint Petersburg, Russia. [8]Ancient DNA Laboratory, Veterinary and Life Sciences School, Murdoch University, 90 South Street, Perth, 6150 Western Australia, Australia. [9]Division of Biology, Kansas State University, Manhattan, 66506-4901 Kansas, USA. [10]Landscape Dynamics Unit, Swiss Federal Research Institute WSL, Zürcherstrasse 111, CH-8903 Birmensdorf, Switzerland. [11]Institut des Sciences de l'Evolution de Montpellier, UMR 5554 Université Montpellier 2, Bat.22, CC061, Place Eugène Bataillon, 34095 Montpellier Cedex 5, France. [12]University of Alaska Museum of the North, Fairbanks, 99775-6960 Alaska, USA. [13]Department of Arctic and Marine Biology, UiT, The Arctic University of Norway, NO-9037 Tromsø, Norway. [14]Genoscope, Institut de Genomique du Commissariat à l'Energie Atomique (CEA), 91000 Evry, France. [15]Adam Mickiewicz University, Faculty of Physics, Umultowska 85, 61-614 Poznań, Poland. [16]Poznań Radiocarbon Laboratory, Poznań Science and Technology Park, Rubież 46, 61-612 Poznań, Poland. [17]Tromsø University Museum, NO-9037 Tromsø, Norway. [18]Centre for Ecological and Evolutionary Synthesis, Department of Biosciences, University of Oslo, P.O. Box 1066, Blindern, NO-0316 Oslo, Norway. [19]Permafrost Laboratory, Department of Geography, University of Sussex, Brighton BN1 9QJ, UK. [20]Institute of Ecology and Evolution, Russian Academy of Sciences, 33 Leninsky Prospect, 119071 Moscow, Russia. [21]Department of Biology, Terrestrial Ecology, Universitetsparken 15, DK- 2100 Copenhagen Ø, Denmark. [22]Australian Centre for Ancient DNA, School of Earth & Environmental Sciences, University of Adelaide, Adelaide, 5005 South Australia, Australia. [23]Department of Geology/Quaternary Sciences, Lund University Sölvegatan 12, SE-223 62 Lund, Sweden. [24]Department of Earth and Atmospheric Sciences, University of Alberta, T6G 2E3 Edmonton, Alberta, Canada. [25]Government of Yukon, Department of Tourism and Culture, Yukon Palaeontology Program, PO Box 2703 L2A, Y1A 2C6 Whitehorse, Yukon Territory, Canada. [26]INRA, UMR1213 Herbivores, F-63122 Saint-Genès-Champanelle, France. [27]Zoological Institute of Russian Academy of Sciences, Universitetskaya nab. 1, 199034 Saint-Petersburg, Russia. [28]Institute of Applied Ecology of the North of North-Eastern Federal University, Belinskogo Street 58, 677000 Yakutsk, Republic of Sakha (Yakutia), Russia. [29]Centre for Archaeological Science, School of Earth and Environmental Sciences, University of Wollongong, Wollongong, 2522 New South Wales, Australia. [30]Division of Vertebrate Zoology/Mammalogy, American Museum of Natural History, New York, 10024 New York, USA. †Present addresses: Centre for Ecological and Evolutionary Synthesis, Department of Biosciences, University of Oslo, PO Box 1066, Blindern, NO-0318 Oslo, Norway (S.B.); Alfred Wegener Institute, Helmholtz Centre for Polar and Marine Research, Research Unit Potsdam, Telegrafenberg A 43, 14473 Potsdam, Germany (L.S.E.); SpyGen, Savoie Technolac, 17 allée du lac Saint André, BP 274, 73375 Le Bourget-du-Lac Cedex, France (E.B.).
*These authors contributed equally to this work.
‡Deceased

For most plant groups, DNA permits identification at lower taxonomic levels than pollen[14]. In addition, environmental DNA records have proven to reflect not only the qualitative but also the quantitative diversity of above-ground plant[12] and animal taxa[9], as determined from modern subsurface soils.

Leaching of DNA through successive stratigraphic zones may be an issue in temperate conditions[9,11] but not in permafrost[6] or in sediments that have only recently thawed[15]. Re-deposition of sediments and organics can confound results, which is also the case for pollen and macrofossils[7,16], but can be avoided and accounted for by careful site selection and by excluding rare DNA sequence reads[16]. For Quaternary permafrost settings, at least, taphonomic bias due to differences in DNA survival across plant groups does not appear to be of concern (see Methods section 4.0 on taphonomy), as has been shown by a comparative permafrost ancient DNA study of plants and their associated fungi[8].

Reconstruction of Arctic vegetation from permafrost

We collected 242 sediment samples from 21 sites across the Arctic (Fig. 1 and Extended Data Table 1). Ages were determined by accelerator mass spectrometry radiocarbon (^{14}C) dating, and are reported here in thousands of calibrated (calendar) years BP (Extended Data Fig. 1 and Supplementary Data 1). We sequenced the short P6 loop sequence of the *trn*L plastid (gene encoding chloroplast transfer RNA for leucine) region and a part of the ITS1 spacer region through metabarcoding (Methods section 3.0), generating a total of 14,601,839 *trn*L plant DNA sequence reads and 1,652,857 internal transcribed spacer (ITS) reads. Reads were identified by comparison with (1) the Arctic *trn*L taxonomic reference library[14], which we extended with ITS sequences for three families; (2) a new north boreal *trn*L taxonomic reference library constructed by sequencing 1,332 modern plant samples representing 835 species; and (3) GenBank, using the program ecoTag (Supplementary Data 2 and Methods section 3.0). Basic statistics, *in silico* analyses, and additional experiments were carried out to check data reliability (Extended Data Fig. 2 and Extended Data Table 2). We grouped the identified molecular operational taxonomic units (MOTUs) into three distinct intervals (Fig. 2a): (1) pre-Last Glacial Maximum (LGM) (50–25 kyr BP), a period of fluctuating climate; (2) LGM (25–15 kyr BP), a period of constantly cold and dry conditions; and (3) post-LGM (15–0 kyr BP), which includes the current interglacial, characterized by relatively higher temperatures[17].

Shifts in plant community composition

To address compositional changes in vegetation across space and time we used a generalized linear model and permutational multivariate analysis of variance (PERMANOVA) (Supplementary Data 3 and Methods section 6.0). We find that (1) the composition of plant MOTU assemblages differed significantly across the three intervals (pseudo-$F = 6.77$, $P < 0.001$, Extended Data Fig. 3a–e), with pre-LGM and post-LGM plant assemblages differing the most (Extended Data Fig. 3f); (2) the greater the spatial distance separating a pair of samples within each time period, the less similar their composition ($P < 0.001$); and (3) LGM assemblages were the most homogeneous across space and post-LGM assemblages were the most heterogeneous (Fig. 2).

LGM pollen spectra show high floristic richness compared to other intervals (for example, ref. 1). This is due to the limited occurrence of woody taxa with high pollen production, which in turn proportionately emphasizes less-productive taxa. By contrast, our DNA data reveal that plant diversity was lowest during LGM relative to other intervals (Fig. 2a). Plant assemblages became more similar to each other and the estimated number of MOTUs decreased from pre-LGM to LGM (Fig. 2a), with many taxa absent that had previously been well represented

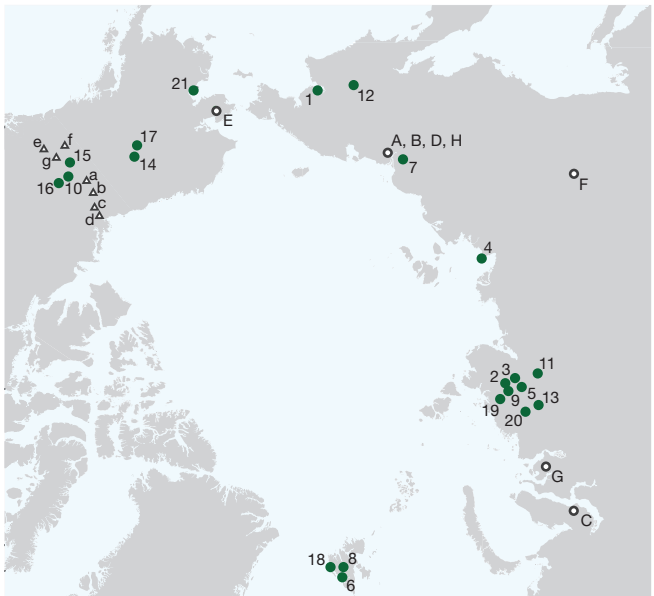

Figure 1 | Sample localities. A total of 242 permafrost samples were collected from 21 sites, shown by green dots (1–21). Eight ancient megafauna gut and coprolite samples (A–H) are shown by grey hollow circles, and seven modern nematode localities are shown by grey hollow triangles (a–g). (1) Anadyr, (2) Baskura Peninsula, (3) Bol'shaya Balakhnaya, (4) Buor Khaya, (5) Cape Sabler, (6) Colesdalen, (7) Duvanny Yar, (8) Endalen, (9) Federov Island, (10) Goldbottom, (11) Khatanga, (12) Maine River, (13) Ovrazhny Peninsula, (14) Purgatory, (15) Quartz Creek, (16) Ross Mine, (17) Stevens Village, (18) Stuphallet, (19) Taimyr Lake, (20) Upper Taymyr River, (21) Zagoskin Lake, (A) Drevniy Creek Mammoth, (B) Bison, (C) Lyuba Mammoth, (D) Kolyma Rhino, (E) Last Chance Creek Horse, (F) Churapcha Rhino, (G) Mongochen Mammoth, (H) Finish Creek Valley Mammoth, (a) Blackstone River, (b) Ogilvie Mountains, (c) Eagle Plains South, (d) Eagle Plains North, (e) Little Atlin Lake, (f) Kluane Lake, (g) Carmacks.

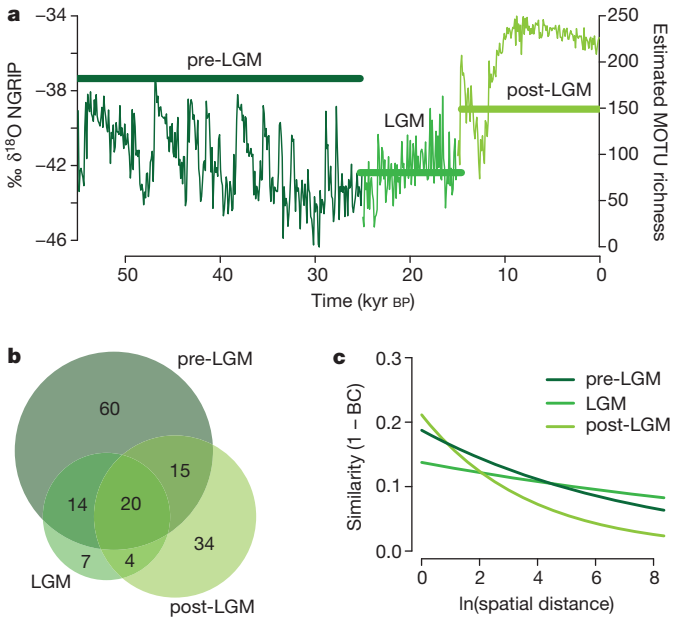

Figure 2 | Taxonomic diversity of Arctic plant assemblages during the last 50 kyr. Taxon composition was estimated by high-throughput sequencing of DNA from 242 permafrost samples. A total of 154 MOTUs were detected. **a**, Index of ambient temperature (continuous line; oxygen isotope concentration, North Greenland Ice Core Project, NGRIP[50]) and estimated MOTU number (horizontal bars; second-order jackknife) are shown for three palaeoclimatic periods: pre-LGM (>25 kyr BP, $n = 149$), LGM (25–15 kyr BP, $n = 32$) and post-LGM (<15 kyr BP, $n = 61$). **b**, MOTU counts recorded uniquely in each palaeoclimatic period and shared among periods. **c**, Modelled decline in similarity (1 − Bray–Curtis (BC) dissimilarity) between pairs of plant assemblages from the same palaeoclimatic period in relation to the spatial distance separating them.

(Fig. 2b). In addition, although the LGM flora was largely a subset of the pre-LGM flora, the post-LGM flora was different (Fig. 2b), with pronounced geographic differentiation (Fig. 2c).

Steppe–tundra

Owing to the low taxonomic resolution of previously published vegetation reconstructions, it remains undetermined whether Arctic vegetation during the last part of the Quaternary was a form of tundra or more like steppe (for example, refs 18, 19). Small-scale contemporary analogues range from low-productivity fellfields and cryoxeric steppe communities to more productive dry Arctic steppe-to-tundra gradients. Our sediment DNA plant sequence data from ~50–12 kyr BP encompass taxa that typify both tundra and Arctic steppe environments. These include taxa that are today typical of dry and/or disturbed sites (for example, *Bromus pumpellianus*, *Artemisia frigida*, *Plantago canescens*, *Anemone patens*), saline soils (*Puccinellia*, *Armeria*), moist habitats (*Caltha*) and rocky or fellfield habitats (*Dryas*, *Draba*), plus a woody component dominated by *Salix* (Supplementary Data 4 and 5). A spatial and/or temporal mosaic of plant communities is indicated (Methods section 6.0), as is seen in floristically rich macrofossil records[4]. The most common MOTU in the pre-LGM and LGM samples is Anthemideae group 1 (*Artemisia*, *Achillea*, *Chrysanthemum*, *Tanacetum*), which underscores the importance in regional pollen assemblages of Asteraceae in general and *Artemisia* in particular[1]. *Equisetum* and *Eriophorum* are important only in postglacial assemblages, reflecting moister soil conditions. Increases in aquatic taxa (Supplementary Data 4 and 5) also indicate a predominance of moister substrates in the later part of the post-LGM period. These findings indicate a shift from dry steppe-tundra to moist tundra in the early part of the post-LGM period—a change widely reported in other proxy studies.

Nematode assemblage composition is known to change with vegetation cover[20], moisture[21] and organic resource inputs[22]. Therefore, to obtain a complementary proxy for vegetation cover and soil quality, we characterized the soil nematode fauna of contemporary mesic shrub tundra and subarctic steppe on well-drained loess soils in Yukon Territory, Canada (Fig. 1 and Extended Data Table 3). The relative proportion of the nematode families Teratocephalidae and Cephalobidae varied among vegetation types ($P < 0.001$, nested ANOVA), and indicator species analysis[23] confirmed that Teratocephalidae (indicator value = 0.98, $P = 0.001$) and Cephalobidae (indicator value = 0.98, $P = 0.001$) are very good indicators of tundra and steppe vegetation, respectively (Fig. 3).

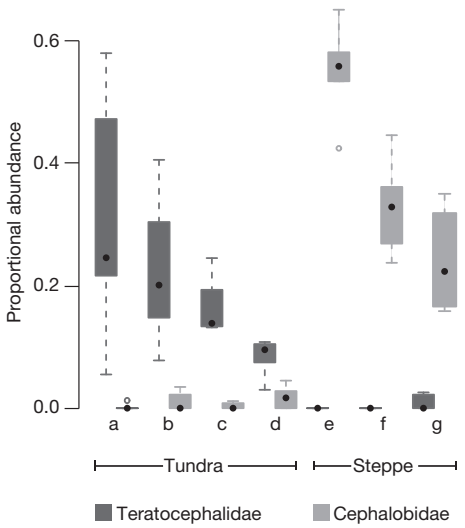

Figure 3 | Proportional abundance of two families—Teratocephalidae and Cephalobidae—among the total soil nematode community at contemporary tundra and steppe sites in Yukon, Canada. Teratocephalidae, dark; Cephalobidae, light. Letters a–g correspond to sample localities (Fig. 1). Median (central dot), quartile (box), maximum and minimum (whiskers) and outlying values (points) are shown.

These findings are in agreement with previous studies restricted to subarctic Sweden[24,25] and alpine and subalpine habitats[26,27]. We amplified short DNA sequences from these two taxa from 17 sediment samples analysed for plant DNA from Yukon and northeastern Siberia. We detected Cephalobidae DNA in almost all samples, whereas Teratocephalidae was detected at a higher frequency in samples younger than 10 kyr BP than in the pre-LGM and LGM samples (Extended Data Table 4). These results support our inferences from plant sequence data and indicate a transition from relatively dry tundra and steppe towards more moist tundra during the post-LGM interval.

Forb dominance and megafaunal diets

To assess structural and functional shifts in the plant assemblages, we investigated temporal changes in the relative abundance of different growth forms. Our DNA results show that pre-LGM vegetation was dominated by forbs, the relative share of which increased during the LGM, whereas graminoids constituted less than 20% of the total read count (Fig. 4a). These results persisted when we corrected for observed modern representational bias[12] (Methods sections 4.0 and 5.3).

Continued forb dominance during the LGM implies that similar proportions of forbs and graminoids were maintained through this period, despite the significant decline in floristic diversity (Fig. 2a, b). Our findings contrast with pollen-based reconstructions, which have emphasized dominance of graminoids in the unglaciated Arctic and adjacent regions, particularly during the LGM, and are exemplified by the widely used term mammoth steppe[19]. Rather, our results show that vegetation was forb-dominated in both overall abundance of MOTUs and in floristic richness (Fig. 4a, b and Extended Data Fig. 3g, h), in agreement with macrofossil data that show a diversity of forbs of mixed ecological preference (for example ref. 4).

We explored whether forbs were prominent in habitats favoured by megafauna by analysing 25 dated (47–20 kyr BP) sediment samples from Main River, Siberia, using *trn*L plastid plant and 16S mitochondrial DNA mammal primers. We found that the mean proportion of forbs was higher in samples from which herbivorous megafaunal DNA had been retrieved ($n = 18$; for example, woolly mammoth, woolly rhinoceros, horse, reindeer and elk) than in samples lacking such DNA ($n = 7$; Fig. 4c and Extended Data Table 5). Although suggestive of co-occurrence of megafauna in forb-dominated settings, these results should be regarded as tentative, and further studies are needed to verify if this is indeed a general trend.

We also investigated whether megafaunal diets revealed the level of forb dominance observed in permafrost sediment samples. Using standardized methods, we genetically characterized intestinal/stomach contents and coprolites recovered from eight specimens of woolly mammoth, woolly rhinoceros, bison and horse from Siberia and Alaska, dated >55–21 kyr BP (Extended Data Table 6 and Methods sections 3.0 and 7.3). Although ingested plant remains are often difficult to identify morphologically, they can be accurately identified[28,29] and roughly quantified[30] using DNA. The majority of these samples are dominated by forbs, which comprise 0.63 ± 0.12 of the sequences, compared to 0.27 ± 0.16 expressing graminoid sequences (Fig. 4d and Supplementary Data 6). These results suggest that megafaunal species supplemented their diets with high-protein forbs rather than specializing more or less exclusively on grasses.

To confirm the reliability of our *trn*L approach for estimating herbivore diet, we analysed 50 rumen samples of sheep-feed diets with varying proportions of forbs (white clover (*Trifolium repens*)) and graminoids (ryegrass (*Lolium perenne*)) (Methods section 5.4). As seen in Fig. 4e, the Pearson correlation coefficient between the actual fraction of forbs in these diets and the proportion of forbs estimated with the DNA-based approach was highly significant ($r^2 = 0.75$, $P < 10^{-15}$).

Discussion

Our observations of high forb abundance in the Terminal Pleistocene may merely reflect vegetation response to glacial climates, but there are

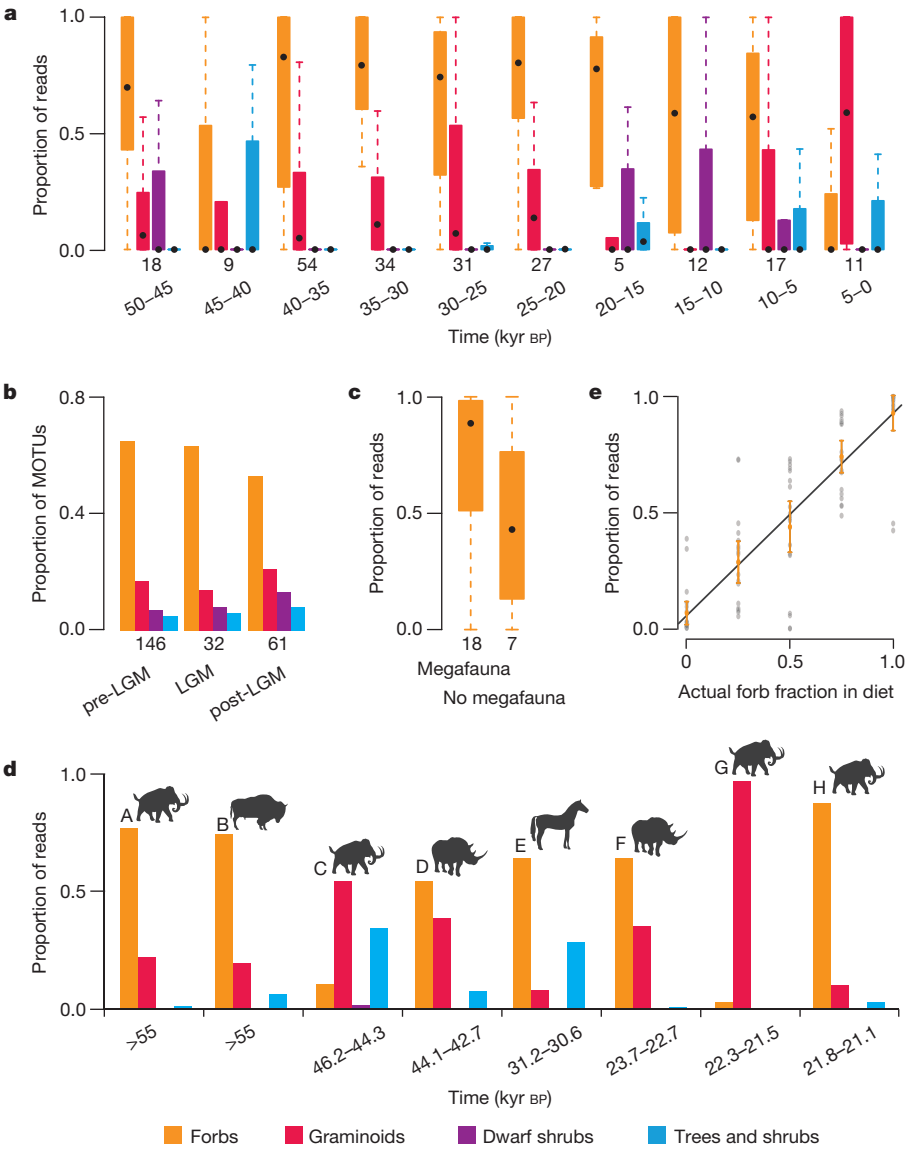

Figure 4 | Plant growth form composition over time and across sample types, estimated by high-throughput sequencing of DNA from 242 permafrost samples. **a**, Proportions of DNA reads corresponding to taxa exhibiting different growth forms, binned over 5 kyr time intervals. The analysis included all sediment samples except 21 Svalbard samples and three further samples for which no growth form information was available. **b**, Number of MOTUs exhibiting different growth forms as a proportion of total MOTU richness in all informative samples for each palaeoclimatic period. **c**, The proportional abundance of forbs in samples from Main River, Siberia (dated 47,100–19,850 yr BP) where megafauna were or were not detected. **d**, Proportions of DNA reads corresponding to different growth forms in megafauna diet, determined from analysis of eight gut and coprolite samples from late Quaternary megafauna species (woolly mammoth, woolly rhinoceros, bison and horse). Letters A–H correspond to the individual samples (Fig. 1). The 95.4% calibrated age range of each sample is shown; '> 55' indicates that the sample was too old to provide a finite radiocarbon age. **e**, Reliability of the *trn*L approach for estimating forb and graminoid abundance in diet analyses. Sheep were fed with known amounts of forbs (*Trifolium repens*) and graminoids (*Lolium perenne*), and the rumen content analysed using the same DNA-based approach as implemented above. Grey dots are raw data points, orange dots and lines represent the means and ± standard errors for diets containing different fractions of forbs. The grey line is a linear model fit. Numbers immediately below the columns in **a**, **b** and **c** indicate sample sizes. Median (central dot), quartile (box), maximum and minimum (whiskers) values are shown in **a** and **c**.

other possibilities[1]. An abundant megafauna would have caused significant trampling[31], enhancing gap-based recruitment[32], which could favour forbs[33]. Coupled with nitrogen input from wide-ranging herbivores[34], forbs may out-compete grasses[35]. Furthermore, a diet rich in forbs may help to explain how numerous large animals were sustained; forbs may be more nutrient-rich (for example, ref. 35) and more easily digested[36] than grasses. However, a feedback loop that maintained nutritious and productive forage and supported large mammalian populations in glacial climate regimes may have been impossible to maintain after deglaciation, as C:N ratios increased with global warming[37], and the potential breakdown of the megafauna–forb interaction would have been exacerbated by declining mammalian populations. In contemporary tundra and steppe (the latter often called grasslands), graminoids are generally perceived to be the dominant growth form in large herbivore habitats (for example, refs 38, 39). Our data, which unearth 50 kyr of Arctic vegetation history, call this perception into question.

METHODS SUMMARY

Plant fragments or soil matrix organics were ^{14}C-dated using accelerator mass spectrometry and measured ages were converted into calendar years[40]. Permafrost sampling, DNA extraction, PCR amplification and taxon identification (for example, ref. 41) followed established procedures. Most vascular taxa are covered by ref. 42, and nomenclature is provided accordingly; for the remaining taxa nomenclature follows ref. 43. Dissimilarity between plant assemblages was quantified using pairwise Bray–Curtis distance[44]. Variation in assemblage dissimilarity was decomposed using PERMANOVA[45] and visualized using non-metric multidimensional scaling[46,47]. We used a distance decay approach[48] and a generalized linear model to model variation in plant community assemblages over space and time. Growth form composition of communities was compiled from species trait databases[49]. Differences in the trait composition of assemblages in adjacent climatic periods were compared to a null model assuming random assortment from the previous interval. Nematode faunas of 35 contemporary sediment samples were morphologically determined. Presence of two indicator families (Teratocephalidae for tundra and Cephalobidae for steppe) was genetically determined in 17 ancient sediment samples. Megafaunal DNA and faeces and gut content were determined genetically following established methods. For a detailed discussion, see Methods.

Online Content Any additional Methods, Extended Data display items and Source Data are available in the online version of the paper; references unique to these sections appear only in the online paper.

Received 24 July; accepted 28 November 2013.

1. Anderson, P. M., Edwards, M. E. & Brubaker, L. B. in *The Quaternary Period in the United States. Developments in Quaternary Science* (eds Gillespie, A. E., Porter, S. C. & Atwater, B. F.) 427–440 (Elsevier, 2003).
2. Murray, D. F. in *Arctic and Alpine Biodiversity: Patterns, Causes and Ecosystem Consequences* (eds Chapin, F. S. & Körner, C.) 21–32 (Springer, 1995).
3. Lamb, H. F. & Edwards, M. E. in *Vegetation History. Handbook of Vegetation Science 7* (eds Huntley, B. & Webb, T. III) 519–555 (Kluwer Academic, 1988).

4. Kienast, F., Schirrmeister, L., Siegert, C. & Tarasov, P. E. Palaeobotanical evidence for warm summers in the East Siberian Arctic during the last cold stage. *Quat. Res.* **63,** 283–300 (2005).
5. Willerslev, E. *et al.* Diverse plant and animal genetic records from Holocene and Pleistocene sediments. *Science* **300,** 791–795 (2003).
6. Haile, J. *et al.* Ancient DNA reveals late survival of mammoth and horse in interior Alaska. *Proc. Natl Acad. Sci. USA* **106,** 22352–22357 (2009).
7. Jørgensen, T. *et al.* A comparative study of ancient sedimentary DNA, pollen and macrofossils from permafrost sediments of northern Siberia reveals long-term vegetational stability. *Mol. Ecol.* **21,** 1989–2003 (2012).
8. Lydolph, M. C. *et al.* Beringian paleoecology inferred from permafrost-preserved fungal DNA. *Appl. Environ. Microbiol.* **71,** 1012–1017 (2005).
9. Andersen, K. *et al.* Meta-barcoding of 'dirt' DNA from soil reflects vertebrate biodiversity. *Mol. Ecol.* **21,** 1966–1979 (2012).
10. Parducci, L. *et al.* Glacial survival of boreal trees in northern Scandinavia. *Science* **335,** 1083–1086 (2012).
11. Haile, J. *et al.* Ancient DNA chronology within sediment deposits: are paleobiological reconstructions possible and is DNA leaching a factor? *Mol. Biol. Evol.* **24,** 982–989 (2007).
12. Yoccoz, N. G. *et al.* DNA from soil mirrors plant taxonomic and growth form diversity. *Mol. Ecol.* **21,** 3647–3655 (2012).
13. Willerslev, E. & Cooper, A. Ancient DNA. *Proc. R. Soc. Lond. B* **272,** 3–16 (2005).
14. Sønstebø, J. H. *et al.* Using next-generation sequencing for molecular reconstruction of past Arctic vegetation and climate. *Mol. Ecol. Resour.* **10,** 1009–1018 (2010).
15. Hebsgaard, M. B. *et al.* The farm beneath the sand—an archaeological case study on ancient 'dirt' DNA. *Antiquity* **83,** 430–444 (2009).
16. Arnold, L. J. *et al.* Paper II - Dirt, dates and DNA: OSL and radiocarbon chronologies of perennially frozen sediments in Siberia, and their implications for sedimentary ancient DNA studies. *Boreas* **40,** 417–445 (2011).
17. Hopkins, D. M. in *Paleoecology of Beringia* (eds Hopkins, D. M., Matthews, J. V. Jr, Schweger, C. E. & Young, S. B.) 3–28 (Academic, 1982).
18. Ritchie, J. C. & Cwynar, L. C. in *Paleoecology of Beringia* (eds Hopkins, D. M., Matthews, J. V. Jr, Schweger, C. E., Young, S. B. & Stanley, V.) 113–126 (Academic, 1982).
19. Guthrie, R. D. *Frozen Fauna of the Mammoth Steppe* (Univ. Chicago Press, 1990).
20. Yeates, G. W. Diversity of nematode faunae under three vegetation types on a pallic soil in Otago, New Zealand. *NZ J. Zool.* **23,** 401–407 (1996).
21. Sohlenius, B. Influence of climatic conditions on nematode coexistence — a laboratory experiment with a coniferous forest soil. *Oikos* **44,** 430–438 (1985).
22. Yeates, G. W. Nematodes as soil indicators: functional and biodiversity aspects. *Biol. Fertil. Soils* **37,** 199–210 (2003).
23. Dufrêne, M. & Legendre, P. Species assemblages and indicator species: the need for a flexible asymmetrical approach. *Ecol. Monogr.* **67,** 345–366 (1997).
24. Ruess, L., Michelsen, A. & Jonasson, S. Simulated climate change in subarctic soils: responses in nematode species composition and dominance structure. *Nematology* **1,** 513–526 (1999).
25. Sørensen, L. I., Mikola, J., Kytoviita, M.-M. & Olofsson, J. Trampling and spatial heterogeneity explain decomposer abundances in a sub-Arctic grassland subjected to simulated reindeer grazing. *Ecosystems* **12,** 830–842 (2009).
26. Popovici, I. & Ciobanu, M. Diversity and distribution of nematode communities in grasslands from Romania in relation to vegetation and soil characteristics. *Appl. Soil Ecol.* **14,** 27–36 (2000).
27. Hoschitz, M. & Kaufmann, R. Nematode community composition in five alpine habitats. *Nematology* **6,** 737–747 (2004).
28. Poinar, H. N. *et al.* Molecular coproscopy: dung and diet of the extinct ground sloth *Nothrotheriops shastensis*. *Science* **281,** 402–406 (1998).
29. Hofreiter, M. *et al.* A molecular analysis of ground sloth diet through the last glaciation. *Mol. Ecol.* **9,** 1975–1984 (2000).
30. Soininen, E. M. E. *et al.* Analysing diet of small herbivores: the efficiency of DNA barcoding coupled with high-throughput pyrosequencing for deciphering the composition of complex plant mixtures. *Front. Zool.* **6,** 16 (2009).
31. Zimov, S. A., Zimov, N. S., Tikhonov, A. N. & Chapin, F. S. I. Mammoth steppe: a high-productivity phenomenon. *Quat. Sci. Rev.* **57,** 26–45 (2012).
32. Owen-Smith, N. Pleistocene extinctions: the pivotal role of megaherbivores. *Paleobiology* **13,** 351–362 (1987).
33. Austrheim, G. & Eriksson, O. Recruitment and life-history traits of sparse plant species in subalpine grasslands. *Can. J. Bot.* **81,** 171–182 (2003).
34. Wardle, D. A. & Bardgett, R. D. Human-induced changes in large herbivorous mammal density: the consequences for decomposers. *Front. Ecol. Environ.* **2,** 145–153 (2004).
35. Güsewell, S. N. P ratios in terrestrial plants: variation and functional significance. *New Phytol.* **164,** 243–266 (2004).
36. Cornelissen, J. *et al.* Leaf digestibility and litter decomposability are related in a wide range of subarctic plant species and types. *Funct. Ecol.* **18,** 779–786 (2004).
37. McLauchlan, K. K., Williams, J. J., Craine, J. M. & Jeffers, E. S. Changes in global nitrogen cycling during the Holocene epoch. *Nature* **495,** 352–355 (2013).
38. van der Wal, R. Do herbivores cause habitat degradation or vegetation state transition? Evidence from the tundra. *Oikos* **114,** 177–186 (2006).
39. Bråthen, K. A. *et al.* Induced shift in ecosystem productivity? Extensive scale effects of abundant large herbivores. *Ecosystems* **10,** 773–789 (2007).
40. Reimer, P. J. *et al.* IntCal09 and Marine09 radiocarbon age calibration curves, 0–50,000 years cal BP. *Radiocarbon* **51,** 1111–1150 (2009).
41. Taberlet, P. *et al.* Power and limitations of the chloroplast *trn*L (UAA) intron for plant DNA barcoding. *Nucleic Acids Res.* **35,** e14 (2007).
42. Elven, R., Murray, D. F., Razzhivin, V. Y. & Yurtsev, B. A. *Annotated Checklist of the Panarctic Flora (PAF)* http://nhm2.uio.no/paf/ (Natural History Museum, Univ. Oslo, 2011).
43. Sayers, E. W. *et al.* Database resources of the National Center for Biotechnology Information. *Nucleic Acids Res.* **37,** D5–D15 (2009).
44. Bray, J. R. & Curtis, J. T. An ordination of the upland forest communities of southern Wisconsin. *Ecol. Monogr.* **27,** 325–349 (1957).
45. Anderson, M. J. A new method for non-parametric multivariate analysis of variance. *Austral. Ecol.* **26,** 32–46 (2001).
46. Shepard, R. N. The analysis of proximities: multidimensional scaling with an unknown distance function. I. *Psychometrika* **27,** 125–140 (1962).
47. Shepard, R. N. The analysis of proximities: multidimensional scaling with an unknown distance function. II. *Psychometrika* **27,** 219–246 (1962).
48. Nekola, J. C. & White, P. S. The distance decay of similarity in biogeography and ecology. *J. Biogeogr.* **26,** 867–878 (1999).
49. Klotz, S., Kühn, I. & Durka, W. *BIOLFLOR* (Bundesamt für Naturschutz, 2002).
50. NGRIP dating group, 2008. IGBP PAGES/World Data Center for Paleoclimatology Data Contribution Series # 2008-034. NOAA/NCDC Paleoclimatology Program, Boulder CO, USA. (2008).

Supplementary Information is available in the online version of the paper.

Acknowledgements We thank A. Lister, R. D. Guthrie, M. Hofreiter and L. Parducci for thoughts and discussions on our findings and K. Andersen for help identifying possible contamination. We thank T. B. Brand, P. S. Olsen, V. Mirré, L. J. Gillespie, J. M. Saarela, J. Doubt, M. Lomonosova, D. Shaulo, J. E. Eriksen, S. Ickert-Bond, T. Ager, D. Bielman, M. Hajibabaei, A. Telka and S. Zimov for help and providing samples. We thank the Danish National Sequencing Centre. This work was supported by the European Union 6th framework project ECOCHANGE (GOCE-2006-036866, coordinated by P.T.), the Danish National Research Foundation (Centre of Excellence to E.W.), the European Regional Development Fund (Centre of Excellence FIBIR and IUT 20-28 to J.D., M.M. and M.Z.), the Research Council of Norway (191627/V40 to C.B.), the Australian Research Council (DP0558446 to R.G.R.), a Marie Curie International Outgoing Fellowship (PIOF-GA-2009-253376 to E.D.L.) and a Carlsberg Foundation Fellowship (to M.V.).

Author Contributions The paper represents the joint efforts of several research groups, headed by various people within each group. Rather than publishing a number of independent papers, we have chosen to combine our data in this paper in the belief that this creates a more comprehensive story. The authorship reflects this joint effort. The ECOCHANGE team designed and initiated the project. E.W., M.E.E., J.M., E.D.L., M.V., G.G., J.H., J.C., I.G.A., P.M., D.F., G.Z., A.T., J.A., A.S., G.S., R.G.R., R.D.E.M., M.T.P.G., A.C. and K.H.K. collected the samples. G.G., R.E., A.K.B., J.H.S., C.B., L.G., E.C. and P.T. constructed the plant DNA taxonomic reference libraries and provided taxonomic assignments of the sediment data with input from I.G.A., E.B., S.B., L.S.E., M.E.E. and D.M. E.D.L., M.V., J.H., L.S.E., S.B., C.C., P.W., L.G., G.G. and J.H.S. conducted the genetics laboratory work. T.G. did the dating. F.P., D.R. and V.N. produced and analysed the data concerning the reliability of the *trn*L approach for estimating herbivore diet. J.D., M.M., M.Z., E.C., M.V., M.R., J.C., S.B., P.B.P., R.C., H.B., R.R., T.M. and P.T. did the analyses. E.D.L. and J.D. produced the figures. E.W. wrote most of the text with input from all authors, in particular J.D., M.M., M.Z., E.D.L., M.E.E., M.V., P.B.P., D.M., K.A.B., N.Y., L.O., C.B., P.T. and R.D.E.M.

Author Information All the raw and filtered data concerning plants, nematodes, megafauna and sheep diet are available either from Extended Data and Supplementary Data, or from the Dryad Digital Repository: http://doi.org/10.5061/dryad.ph8s5. Reprints and permissions information is available at www.nature.com/reprints. The authors declare competing financial interests: details are available in the online version of the paper. Readers are welcome to comment on the online version of the paper. Correspondence and requests for materials should be addressed to E.W. (ewillerslev@snm.ku.dk).

METHODS

1.0 Sites and sediment sampling. Site details and related publications are provided in Extended Data Table 1. The sampled sites are generally well characterized stratigraphically, but not all details are published. Complete site and sample information is available from the ECOCHANGE database manager (H.A.Binney @soton.ac.uk) and the Dryad database (also see section 8 for further details on sites). The samples are of mixed provenance: the majority of samples representing the pre-LGM ($n = 149$) and LGM ($n = 32$) come from exposures of frozen 'ice-complex' deposits, in which the clastic component (silt and fine sand) derives mainly from aeolian deposition and surface runoff in terrestrial permafrost settings characterized by ice-wedge polygons, whereas most of the post-LGM samples ($n = 61$) come from modern soil and peat (37%), aeolian sediment (30%), thermokarst-lake infill (13%) and fluvial terrace (11%) sequences, and a few samples of mixed origin (9%). In most cases, frozen sediment samples were extracted by horizontal drilling using established protocols to guard against sample-based contamination[5,7,51,52] and were kept frozen until they were processed for DNA analyses. A list of samples and age estimates is given in Supplementary Data 1. Some of the samples are used in earlier studies[6,7,16].

In July 2009 we sampled soil from sites representing moist tundra and steppe vegetation from seven different locations in Yukon Territory, northwestern Canada (Extended Data Table 3). Intact soil cores were excavated in 15 or 30 cm (depending on depth of the A-horizon or the active layer over the permafrost) PVC tubes with a 5-cm diameter inserted into a hollow steel auger forced vertically into the ground. PVC tubes were closed with close-fitting lids and transported in an electric cooler to Whitehorse, where they were temporarily stored at 5 °C before they were shipped to Centre for GeoGenetics, University of Copenhagen, for processing. From each soil core the five top and bottom cm were processed. In addition, the moss layer, when present, was processed from tundra samples. Sample material from each layer was homogenized before subsamples were taken for nematode extraction. Bulk density varies greatly between moss, peat and soil, hence the weight of extracted fractions vary between the different sample materials. Nematodes were extracted from 2.0–10.0 g of sample material for 48 h by a modified Baermann tray method[53]. Nematodes were heat-fixed (80 °C) in 4% formaldehyde, and a minimum of 100 individuals per sample was identified to genus or family using a compound microscope at ×1,000 magnification.

Ancient megafauna intestinal/stomach contents and coprolites were collected directly from permafrost and from permafrost-preserved animals (Extended Data Table 6). Interior parts were sampled for DNA analyses.

2.0 Chronology methods. For the majority of samples, plant fragments and soil matrix organics extracted from sediment samples using protocols described in, for example ref. 54, were radiocarbon-dated using accelerator mass spectrometry. ^{14}C ages were calibrated with the IntCal09 calibration curve[40], or (in the case of modern or near-modern soil samples) using the record of post-bomb atmospheric ^{14}C concentrations. Modern samples yielded ^{14}C concentrations over 100 pMC (per cent modern carbon) that matched variations in the twentieth century atmospheric carbon related to nuclear testing and other enrichment[55]. In cases where a series of ages from one profile was available, age-depth models were calculated, using the free-shape algorithm published in ref. 56, allowing undated samples to be assigned ages. Age models were only applied to sequences for which stratigraphic evidence supported continuous accumulation of sedimentary units. For a few sequences with previously ascribed dates, calibrated ages were assigned on the basis of the calibration routine available at http://www.neotomaDB.org. ECOCHANGE radiocarbon ages and supporting information are contained within the dating table of the ECOCHANGE meta-database (see above).

3.0 DNA extraction, amplification and sequencing. DNA extraction of permafrost samples and coprolites and intestinal/stomach contents followed the protocols of refs 6, 57, 58. For construction of the new northern boreal plant reference library, DNA was extracted from leaves taken from taxonomically verified museum specimens originating from across the circumboreal region and sequenced for the plastid *trn*L intron, following the protocols of ref. 14.

3.1 Amplification of plant DNA from sediments. For the ancient plant DNA from sediments, PCR amplification was done in Grenoble using nine base pair (bp)-tagged generic plant primers[41] for the P6 loop of the *trn*L plastid region (*gh* primers). We did not use the two standard barcoding markers *rbc*L and *mat*K in this study, despite the extensive reference database available, as they are not appropriate for working with degraded DNA, as demonstrated in ref. 12. First, these markers are too long (c. 500 bp for *rbc*L and 800 bp for *mat*K) for reliably amplifying degraded DNA, and second, it is not possible to shorten them by designing versatile primers on protein-coding genes. Hence some amplification products can be obtained, but with a strong bias among plant groups according to the variations of the primer target sequences.

Each *trn*L tag was distinguished from any other tag by at least three base differences. The list of tags was generated using the oligoTag program[59]. In order to increase the taxonomic resolution of the analysis for three plant families, three additional primer pairs were used (F, forward primer; R, reverse primer): ITS1-F, GATATCCGTTGCCGAGAGTC[60]; ITS1Poa-R, CCGAAGGCGTCAAGGAAC AC[60]; ITS1Ast-R, CGGCACGGCATGTGCCAAGG[60]; ITS1Cyp-R, GGATGAC GCCAAGGAACAC (this study). They target ITS1 of nuclear ribosomal DNA in Poaceae (ITS1-F and ITS1Poa-R), Asteraceae (ITS1-F and ITS1Ast-R) and Cyperaceae (ITS1-F and ITS1Cyp-R). These primers were tagged in the same way as the P6 loop primers to allow the assignment of sequence reads to the relevant sample. PCR conditions followed the protocol of ref. 12. Each permafrost and modern soil sample was amplified five times with the *gh* primer pair and once with each of the ITS1 primer pairs. Amplicons were sequenced using the Illumina GA IIx platform as 2 × 108-bp paired-end reads.

3.2 Amplification of plant DNA from coprolites and intestinal/stomach contents. DNA amplifications were carried out in Copenhagen with the *trn*L *gh* primers[41] with multiplex identifier (MID) incorporated tags. For each sample, PCR was carried out twice with the same-tagged primers and with the use of HiFi (Invitrogen) polymerase and 5 µl of extract with 50 cycles of PCR. PCR products were pooled equimolarly and subsequently sequenced on the Roche FLX DNA sequencing platform (Copenhagen) following previously established protocols[12]. 16SMamm1 and 16SMamm2 primers[61] were used to PCR amplify DNA from the environmental faeces extracts, and the amplicons cloned in order to identify the species of origin.

3.3 Amplification of megafauna DNA from sediments. For megafauna DNA in permafrost, PCRs were performed in the ancient DNA laboratory of the Natural History Museum at the University of Oslo, using the 16Smam1 and 16Smam2 primers[61] and a human-specific blocking primer (16Smam_blkhum3 (ref. 57)). Fusion primers containing the Lib-L forward and reverse primers (Roche 454) were used, and 16Smam1 included a MID sequence to allow multiplexing of PCR products for sequencing. PCR mixture and profile were as described in ref. 57. All samples, including extraction blanks, were amplified a maximum of six times in an attempt to obtain two positive PCR replicates, where positive PCRs are those that produced a visible band of the correct size on an agarose gel. When successful, the two PCR replicates were combined, and purified and normalized together using SequalPrep Normalization plates (Invitrogen).

The purified PCR products were sequenced on three machines following the manufacturer's guide for amplicon sequencing. All the plant *trn*L introns and ITS products were sequenced on the Illumina GA IIx platform, the Norwegian Sequencing Centre was used for sequencing of megafauna DNA (Roche 454 GS FLX Titanium).

3.4 Amplification of nematode DNA from sediments. For nematodes, PCR amplification, carried out in Copenhagen, was attempted on a subset of samples using two primer sets. The Cep (forward primer CepF, 5′-CCGATAACGAGC GAGACTC-3′; reverse primer CepR, 5′-CGGCTAAACACCGAAATCC-3′) and Ter (forward primer TerF, 5′-GCTCTCAAGGTGTATATCGC-3′; reverse primer TerR, 5′-AAACCAGCAGTATTAGCC-3′) primers target a 90-bp region of the 18S ribosomal DNA of the Cephalobidae and a 118-bp region of the 18S rDNA of the Teratocephalidae, respectively. All primers were flanked by the Lib-L forward and reverse primers (Roche 454), and the 5′ primers were further flanked by an 8-bp DNA tag[62]. PCRs were performed with 2 µl template DNA in a mixture described in ref. 7 under the following conditions: initial denaturation at 94 °C for 5 min, followed by 65 cycles of denaturation at 94 °C for 30 s, annealing at 52 °C or 50 °C for Cep and Ter primers, respectively, for 30 s, and extension at 68 °C for 30 s. Cycling was completed at 72 °C for 7 min. PCR products of the correct size (checked on a 2% agarose gel) were purified using the QIAquick Gel Extraction Kit (Qiagen) according to the manufacturer's protocol. PCR reactions were repeated at least three times; five times for samples that failed to produce amplicons using either of the primer pairs.

4.0 Taphonomy and contamination issues. The need to understand the taphonomy of a palaeo-proxy system has recently been emphasized[63]. Here we further assess taphonomic bias and possible contamination of the samples. Fossil assemblages do not represent life assemblages exactly owing to post-mortem processes, including differential decomposition, depositional changes and addition or removal of material[64]. Our landscape-scale taphonomic model for plant DNA derives it from *in situ* burial of above- and below-ground plant parts, downslope transport of material in above-ground and below-ground flow as particles or with DNA as part of soil–water colloidal complexes, and possible deposition from a vector such as animals or wind. Tests in Svalbard (ECOCHANGE, unpublished data) indicate that local (3–50 m^2) sources provide almost all plant DNA in modern soils.

For yedoma, the surface vegetation was rooted in an accreting substrate that had insufficient time for full profile development before burial and freezing (for example, inceptisols; see ref. 65). The active layer (estimated at ~50 cm for the LGM of Alaska[65]) acts as a time-averaging moving window, with penetration of unfrozen material to a level by roots potentially occurring until the freezing front reaches that level. We estimate that most yedoma samples record DNA over

~1,000 years of accumulation, but with a bias towards the first few hundred years, based on observations of how deeply roots penetrate modern soils and average accumulation rates of sediment. We also tested for differences in accumulation rate between time periods that might lead to bias in diversity estimates[66] (Supplementary Data 1). There was no significant difference between pre-LGM and LGM rates (1.12 and 1.25 mm yr^{-1}, respectively). The post-LGM had significantly greater average rates (3.82 mm yr^{-1}), but this estimate is based on only a few sites and samples and more diverse forms of sedimentation; furthermore, beta diversity increases, rather than diminishes, as would be expected if there were bias, in the post-LGM. We conclude that time-averaging effects in our samples have not biased the diversity estimates.

Peat and lacustrine sediment samples will have finer (decadal) temporal resolution as demonstrated by numerous other proxy studies, and the loess-derived sediments sampled beneath the rapidly deposited Dawson tephra at Quartz Creek (see section 8.3) may be time-averaged over only decades or centuries. The few samples drawn from thermokarst lake deposits could potentially include a wider age range of material derived from lake-bank collapse, but the Holocene ^{14}C chronologies suggest that these sequences can be reliably compared with the Late Pleistocene records.

Ref. 12 showed that graminoid DNA occurs in soil in about the same proportions as graminoids occupy the above-ground biomass. We might expect woody plants to release environmental DNA at a lower rate in relation to their above-ground biomass as much of their production goes into woody stems and roots, which have a relatively slow rate of decomposition. Woody biomass may be under-represented in the DNA record by a ratio of approximately 5:1 in comparison with the biomass of non-woody taxa[12]. Pollen and macrofossil data from numerous sites (including our own) attest to the rarity of woody taxa in the pre-LGM and LGM periods. In these two periods, woody taxa are likely under-represented in our DNA record, but even allowing for this they still form a minor component of all assemblages.

Forbs are represented in DNA at a ratio of about 2:1 compared with above-ground biomass (ref. 12). This difference may reflect different litter turnover rates; graminoids are richer in lignins than are forbs[67]. Alternatively, forbs may invest resources into below-ground parts if they are perennials whereas others (not many in the Arctic) are annuals and largely decompose every year, yielding a range of root-shoot ratios[68]. It is unlikely that differential preservation of ancient forb tissue has occurred because this would predict a lessening of forb dominance through time; rather there is continuous forb dominance through the pre-LGM and LGM and an abrupt diminution of forb DNA in the post-LGM. Further, there is no bias in the length of sequences recovered through time (see below), which could otherwise conceivably generate a bias as some of the longer *trn*L sequences occur in the Cyperaceae.

Established protocols for permafrost sampling were followed to control for sample-based contamination[5,6,7,51,52]. All ancient pre-PCR work (that is, subsampling, extraction and PCR setup) was conducted in full body suits in state-of-the-art dedicated ancient DNA laboratories in Copenhagen and Oslo that are physically separated from any other biological laboratories, with positive air pressure and nightly ultraviolet exposure of surfaces, and equipped with positive flow hoods. Occasionally, common contaminants were detected: *Homo sapiens*, *Mus musculus*, *Sus*, *Bos*, *Canis*, *Felis catus*, *Solanum lycopersicum*, *Zea mays* and *Cedrus*. The current library preparation protocol cannot fully prevent the production of chimaera sequences between individually tagged PCR products and does not allow contamination of individually tagged PCR products to be detected. To mitigate this problem we used the same tag on each side of the PCR products, allowing the detection of chimaeric products during the library enrichment step (PCR products with different tags on each side were all removed by the ngsfilter program from the OBITools package (http://metabarcoding.org/obitools). Furthermore, we also removed haplotypes which have previously been detected as contaminants in PCR reagents, are exotic to the study sites, or represented likely artificial diversity caused by sequencing errors of contaminant or exotic haplotypes. The taxonomic assignment of these sequences includes Rutaceae, Solanaceae, Solanoideae, Loasaceae and Musaceae. In addition, the following plant MOTUs occurred in sequencing blanks: Salicaceae (group 1), containing *Populus* and *Salix*; *Equisetum* (group 2), containing *E. arvense*, *E. sylvaticum* and *E. fluviatile*; and *Taraxacum*. These MOTUs are likely to genuinely occur in the study samples but were excluded as a conservative measure. We also note that Eritrichium, (group 1), Triticeae (group 1; containing *Elymus* spp., *Leymus* spp.), Apiaceae (group 1), *Betula* (group 1) and *Dryas* (group 1), although not found in the blank controls of this study, have been recorded as possible sources of contamination in other studies. The full list of MOTUs included in the analyses is presented in Supplementary Data 2, 4 and 5.

Importantly, to avoid possible contamination from re-deposition of organics or DNA in the exposures sampled, we did not include any low-abundance sequences in the analyses (see below), as such sequences may be due to re-deposition of material[16].

For further evidence of reliability of results and their interpretations please see section 5.3.

All the raw and filtered data concerning plants, nematodes and megafauna are available either from Extended and Supplementary Data, or from the Dryad Digital Repository (http://doi.org/10.5061/dryad.ph8s5).

5.1 DNA reference libraries. We identified plant sequences retrieved from the ancient samples taxonomically using (1) the Arctic plant *trn*L reference library developed in ref. 14, comprising 842 species representing all widespread or ecologically important taxa of the circum-Arctic flora; (2) a new extension of this library constructed by sequencing the nuclear ribosomal ITS1 region to improve species resolution in three families (Cyperaceae, Poaceae and Asteraceae); (3) a new north boreal plant *trn*L reference library constructed by sequencing DNA extracted from 1,332 herbarium specimens representing 835 of the most common north circumboreal species, of which most also occur in present-day Arctic vegetation; and (4) the EMBL database for sequences not matching taxa contained in these three reference libraries. The specimens used to construct the new north boreal library were sampled after taxonomic verification from the following collections: Herbarium of the Natural History Museum, University of Oslo, Norway (O); Popov Herbarium, Siberian Central Botanical Garden, Novosibirsk, Russia (NSK); National Herbarium of Canada, Canadian Museum of Nature, Ottawa, Canada (CAN); and University of Alaska Museum of the North (ALA). Quality checking and cleaning of this new library was performed by comparing all sequences with published sequences using NCBI/BLAST and by phylogenetic analyses of each family, including sequences from closely related taxa to verify taxonomic identity. All reference databases are available from the Dryad Digital Repository (http://doi.org/10.5061/dryad.ph8s5).

5.2 Sequence groupings and identifications of sedimentary plant DNA. For plant DNA data obtained from the sediment samples, each pair of reads was assembled to reconstruct full-length marker sequence using the illuminapairedend program from the OBITools package (http://metabarcoding.org/obitools). Sequences were associated with their corresponding sample according to the primer tags, and identical sequences were clustered to form MOTUs. MOTUs occurring less than five times in the whole data set or containing ambiguous base symbols were discarded. Only PCR repeats with more than 1,000 sequences for the *gh* primers and 500 sequences for the ITS1 primers were considered for the following process. For *gh* PCR amplification, a MOTU was considered as belonging to a sample if it occurred in the majority of the usable repeats for this sample. Taxonomic assignment of MOTUs was done with the ecoTag program[12] using our plant reference libraries as reference databases: Only MOTUs having at least 95% similarity with a sequence in one of the reference libraries or in the EMBL database were kept in the final data set. Identifications realized with our reference libraries were given priority over EMBL. The final set of MOTUs associated with a sample was based on all MOTUs retrieved from all repeats of this sample. Initial identifications to the species level were in some cases adjusted to a higher taxonomic level based on the completeness of our reference libraries. Most vascular taxa are covered by ref. 42, and nomenclature is provided accordingly. For the remaining taxa nomenclature follows ref. 43. Results are listed in Supplementary Data 2, 4 and 5.

5.3 MOTU characterization and data consistency. Basic statistics were used to check data consistency among time periods. Results are presented in Extended Data Fig. 2a–c, and clearly show that older samples did not present any bias compared with more recent samples. A bias could have been introduced (1) if the size of the *trn*L P6 loop would have been smaller in taxa identified in older samples; (2) if the number of identified taxa were smaller in older samples; or (3) if the number of sequence reads were lower in older samples. This was not the case and we conclude that the reconstructed plant assemblages from different time periods did not suffer from such biases.

We also checked whether the primers used could explain the differences observed between forbs and graminoids. The WebLogos[69] presented in Extended Data Fig. 2d show that the target sequences of the *trn*L *gh* primers[41] are very well preserved in the main families leading to the estimation of the relative proportions of forbs and graminoids. According to the very good match of the *gh* primers in the different families, it is highly unlikely that these minor differences can produce any significant bias in the observed proportions of forbs and graminoids.

Finally, we carried out length statistics of the P6 loop of the *trn*L intron for several plant families (Extended Data Table 2), knowing that shorter sequences are likely to be preferentially amplified over longer sequences. According to the mean length in the different families, Cyperaceae (graminoid) might be under-represented in our results, and Plumbaginaceae (forb) and Polygonaceae (forb) over-represented. In any case, the bias was identical for all samples (permafrost and diet), and for all periods as no size difference among the amplified sequences were observed among period (Extended Data Fig. 2a–c). For all the other families, the size difference is minor, and is unlikely to generate any significant bias.

5.4 Reliability of the *trn*L approach for estimating the diet of herbivores. To test the reliability of the *trn*L approach for estimating the diet of herbivores, we conducted an experiment on sheep. During the period of May–July 2011, pure plots of white clover (*Trifolium repens*, cultivar Merwi) and ryegrass (*Lolium perenne*, cultivar Aberavon) were used to test five mixtures of green fodder (that is, five diets differing by their clover:ryegrass ratios of 0:100, 25:75, 50:50, 75:25 and 100:0).

The five diets were allocated to five 1-year-old male Texel sheep fed ad libitum according to a 5 × 5 Latin square design. For each sheep and each diet, one rumen sample was collected on two successive days. The collection started 13 days after the beginning of the diet in order to prevent an effect from the previous diet. Each of the 50 samples consisted of about 5 g of rumen content.

Total DNA was extracted from about 25 mg of rumen content with the DNeasy Blood and Tissue Kit (QIAgen) following the manufacturer's instructions. The DNA extracts were amplified with the *trn*L *gh* primers (*g* primer, GGGCAATCC TGAGCCAA; *h* primer, CCATTGAGTCTCTGCACCTATC[41]) targeting a short portion of the *trn*L intron of the chloroplast DNA. For each sample two independent PCR replicates were carried out. Paired-end sequencing (100 nucleotides on each extremity of the DNA fragments) was carried out at the French National Sequencing Centre (CEA Genoscope) on an Illumina HiSeq 2000 (Illumina).

A total of 216,586 and 163,328 sequence reads corresponded to *Trifolium repens* (forb) and to *Lolium perenne* (graminoid), respectively. The Pearson correlation coefficient between the actual fraction of forb in diet and the proportion of forb estimated using the DNA-based approach is highly significant ($r^2 = 0.75$, $P < 10^{-15}$) (Fig. 4e).

The experimental procedures were conducted in accordance with French regulations for the use of experimental animals (statutory order no. 87–848, guideline April 19, 1988). All the data concerning the sheep diet experiments are available from the Dryad Digital Repository (http://doi.org/10.5061/dryad.ph8s5).

6.0 Analysis of MOTU assemblage data. Each sediment sample provided a molecular characterization of a local plant assemblage. To analyse gross changes in plant assemblages through space and time we used 242 dated samples from 21 sites (56 entities, that is, individual sections), which provided a total of 7,738,725 chloroplast *trn*L (UAA) intron reads. For these analyses we used only the MOTUs identified with the *gh* primers (see Section 3.0), because the reads of these MOTUs are proportional to vegetation (see ref. 12). In total, 154 taxa (MOTUs) were identified, of which 47 were assigned to species level (Supplementary Data 4). Supplementary Data 5 lists the MOTUs and constituent taxa for the ITS identifications.

6.1 Temporal classification of samples and data robustness. Each sample was allocated to one of three broad age categories: (1) 50–25 kyr BP (pre-LGM), a period of fluctuating climate[70]; (2) 25–15 kyr BP, the LGM, a period of constant cold and dry conditions[17]; (3) 15 kyr BP–present, the current interglaciation (post-LGM), which, subsequent to deglacial warming, is characterized by climate stability and relatively high temperatures[70]. Our specification of LGM timing represents a period between the transition of Marine Isotope Stage (MIS) 3 to MIS 2 and the transition to the Bølling (Gi-1e). This time window incorporates the period of lowest global sea level, which is traditionally used to define the LGM (22–18 kyr BP), along with flanking periods during which the development of glaciation or deglaciation occurred. The use of a fairly wide window was also intended to allow for some regional variation in the timing of the maximum. We assessed the robustness of our analyses to alternative definitions of LGM timing using PERMANOVA[45] (implemented using R package vegan[71]) to test the fit of models including LGM specifications with different duration and timing, falling in the range 30–11 kyr BP. In general, there were not large differences between many of the alternative definitions, and all detected the large shifts in plant assemblages occurring around that time (Supplementary Data 3). To assess whether our temporal definition of post-LGM masked changes before and including the onset of the Holocene at ~11 kyr BP, we extracted the post-LGM subset of data, that is, 15–0 kyr BP, and used PERMANOVA to test whether splitting the data into two time periods (15–11 and 11–0 kyr BP) improved the fit. The results indicated that given the data we have, the split of post-LGM into two consecutive time bins did not significantly improve the null model ($P = 0.08$).

We compared our approach of defining a priori groups based on radiocarbon dating with an unsupervised approach whereby variation between samples was used to define groups. To partition samples into clusters we used k-means clustering with the Hartigan–Wong algorithm, values of k between 2 and 10 and 100 random starting configurations for each value of k. The Calinski–Harabasz criterion was used to identify the best supported values of k[72]. The results of unsupervised clustering largely coincided with our supervised analysis (Extended Data Fig. 3a–d). The two- and three-cluster solutions, which were best supported, revealed the clearest distinction between post-LGM communities on one hand and pre-LGM and LGM samples on the other. This is in accordance with our diversity analysis, which showed that that the species list of the LGM was essentially a subset of the pre-LGM species list, although considerably fewer species were recorded from LGM samples. The higher values of k indicated more subtle differences between LGM and pre-LGM samples.

As a further investigation of data robustness, we repeated the analyses, but imposed an upper limit of 40 kyr BP to the pre-LGM period and excluded older samples, thus equalizing the duration of the pre- and post-LGM periods (both 15 kyr BP). The results of these analyses were qualitatively identical to those based on the whole data set. However, although MOTU richness remained highest in the pre-LGM in the equalized analysis, it was less clearly so (equalized analysis: total richness: pre-LGM = 103, LGM = 48, post-LGM = 74; jackknife second order estimator: pre-LGM = 169, LGM = 85, post-LGM = 159).

6.2 Functional characterization of molecular taxa. We characterized MOTUs in terms of their coarse growth form; 147 of the 154 taxa identified could be placed into four primary groups: forbs, graminoids (grasses plus sedges plus rushes), dwarf shrubs or other woody plants (that is, shrubs and trees). Information on growth form was derived from BiolFlor, a database covering more than 60 plant species traits for 3,659 plant species from the German flora[49,73]. Where data were lacking, we excluded the taxon from analysis.

6.3 Assemblage variation in time and space. Variation in assemblage characteristics among time periods was visualized using two-dimensional nonmetric multidimensional scaling (NMDS)[46,47]. The composition of samples was estimated by the proportion of reads corresponding to particular MOTUs.

Dissimilarity between pairs of plant assemblages was defined using Bray–Curtis dissimilarity[44]. For some analyses similarity was calculated as 1 − BC. Bray–Curtis dissimilarity is frequently used in plant community ecology and is recommended by several basic sources owing to its properties (ref. 74 and elsewhere[71,75,76]). In particular, Bray–Curtis shows a good ability to mirror environmental distances[74,77]. The Bray–Curtis index also works well with proportional abundance data[77,78]. Euclidean distance is also widely used with proportional abundance data. Whereas so-called proportion indices like Bray–Curtis depend on the number of shared species and thus measure distance as proportions of the maximum distance possible, Euclidean distance concentrates only on differences in relative proportional abundances[79]. Thus, the choice of distance measure depends on the emphasis of a particular study, for example, how much attention is paid to different aspects of community assemblage structure. We considered the co-occurrence of taxa in samples to be an important feature of palaeocommunity assembly, and this is why Bray–Curtis was our primary choice. However, as Euclidean distance could add another aspect of community assembly, we performed a parallel analysis (PERMANOVA, NMDS and distance decay) using Euclidean distance. We found that our quantitative results and the qualitative patterns were robust to the choice of distance measure.

First, the ordination was conducted for the whole data set. Second, as the spatial distribution of the total data set was not balanced between time periods, we identified four replicated locations (two in North America, one in western Siberia, one in eastern Siberia) where samples were collected from sites within 100 km of each other in all palaeoclimatic periods. We based a further ordination on an equal number of samples per location per period (15 samples per period, 45 samples in total). Because the results of analyses based on the two data sets coincided, only the results of the first analysis are presented, except in Extended Data Fig. 3e where it was impossible to portray all 242 samples and the results of the second analysis are presented. Stress values for the ordinations were in the range 0.05–0.17. PERMANOVA was used to compare the similarity of floristic composition in different periods.

6.4 Richness estimation. Nonparametric richness estimators are usually recommended owing to their precision and low susceptibility to sampling bias[80]. In particular, the second-order jackknife has been shown to be one of the most effective estimators[81,82], especially for highly sparse palaeontological data[83]. We used the second-order jackknife to estimate species richness in climatic periods.

6.5 Distance-decay measures. We modelled variation in plant communities using a distance-decay in similarity approach[48], using as a dependent variable all pairwise similarities between samples in terms of floristic composition. We used a generalized linear model to describe variation in the dependent variable. The dependent variable was bounded by zero and contained a large proportion of exact zeros (that is, achieved when pairs of samples contained no shared taxa). The data were also theoretically bounded by 1, but in practice no samples were identical and the data exhibited a strong positive skew. To adequately model variation in such a dependent variable, we used a compound Poisson error distribution (using R package tweedie[84]), with an index parameter for the power variance function of 1.45 (estimated using maximum likelihood) and a log link function. The geographic distance separating points was included as an independent variable. This distance was calculated as the natural logarithm of the orthodromic distance between points, that is, calculated as the shortest earth-surface distance between two sets of latitude and longitude coordinates (the earth was assumed to be spherical with a radius of

6,371 km). The second independent variable consisted of a categorical variable representing the combination of the time periods being compared. Thus, this variable had six levels, consisting of all pairwise combinations between these periods (pre-LGM versus pre-LGM, pre-LGM versus LGM, pre-LGM versus post-LGM, and so on).

An interaction term between the independent variables was included in the model. As each sample was represented multiple times in the data set, observations were not independent, biasing model estimates of variance and statistical significance. To estimate the true significance of model terms, we recalculated each model a further 999 times using data sets where the community data underlying the dependent variable were randomized (values were permuted within samples using the permatfull function from the R package vegan). The change in deviance associated with dropping a term in the empirical model was then compared to the corresponding statistics derived from randomized models; significance was estimated based on the number of randomized statistics higher than the empirical value.

6.6 Randomization tests used to assess functional changes between time periods. We used a randomization procedure (BC_{diff}; described in ref. 85, in which BC denotes Bray–Curtis similarity) to assess whether the growth form composition of plant communities of the LGM and post-LGM (target) periods represented a random sample from the directly preceding (source) period. To do this we calculated the Bray–Curtis similarity between the observed mean growth form composition of the target period and each of 999 means derived from a bootstrapped selection (sampled with replacement; the sample size corresponding to that of the target period) of samples from the source period (BC[observed versus random] = BC_{or}). In parallel, BC was calculated 999 times between two random means, calculated as described above (BC[random versus random] = BC_{rr}). The latter calculation provided a population of BC measures that might be expected to arise by chance. The vector of 999 BC_{rr} values was subtracted from the vector of 999 BC_{or} in a random pairwise manner to produce a final vector of 999 values ($BC_{diff} = BC_{or} - BC_{rr}$). BC_{diff} has an expected value of 0 if community composition is random.

This approach indicated that LGM growth form structure did not differ from a random draw from the pre-LGM community (95% quantiles of BC_{diff}; LGM: -0.14–0.11). However, post-LGM growth form composition was not a random subset of that from the LGM (95% quantiles of BC_{diff}: 0.05–0.30). The abundance of forbs decreased whereas the abundance of all other growth form types increased in the post-LGM compared with the LGM period (Extended Data Fig. 3g).

6.7 Overview of vegetation change through time. We classified a subset of samples (those of finite age) into 5,000-year age classes (from 50–45 to 5–0 kyr) across the region encompassing central and northeast Siberia and Alaska–Yukon. These regions were unglaciated and inhabited by the megafauna in the Pleistocene, and they are the regions from which the dietary samples originated. The samples from Svalbard used in the previous analyses were omitted here as Svalbard was almost entirely glaciated in the LGM and did not host megafauna. We plotted the abundance of the key groups (described above) as estimated by the abundance of DNA sequence reads through time to provide an overview of their shifting importance. We also calculated the number of MOTUs detected for each group through time (Extended Data Fig. 3h).

7.1 Nematode data. Nematode sequences were sorted according to the DNA tag used. Within individual PCR products, sequences represented by less than five reads were discarded. The remaining sequences were assigned to taxa using the statistical assignment package SAP[86].

We used Dufrêne–Legendre indicator species analysis[23] to identify nematode taxa that acted as good indicators of modern tundra or steppe habitat (as implemented by the indval function from the R package labdsv[87]). The function calculates an indicator value for each taxon that is the product of its relative frequency and relative average abundance in sample groups (the groups in this case being steppe and tundra). The value varies from 0 to 1 and would be maximal if all examples of a taxon were distributed among all samples from only one of tundra or steppe. By morphologically determining the nematode faunas of 35 sediment samples from contemporary tundra and steppe sites in Yukon, Canada, we discovered two indicator families: Teratocephalidae for tundra and Cephalobidae for steppe. We tested whether the proportion of the two families differed between tundra and steppe with a nested ANOVA (site nested within vegetation type) (SAS Enterprise Guide, version 4). Data on proportions were square root transformed to obtain homogeneity of variance (Bartlett test). The ANOVA was executed on non-normally distributed data, but the ANOVA is quite robust to non-normality[88]. We genetically determined the presence of the two indicator families in 17 of the 242 ancient sediment samples; results are listed in Extended Data Table 4.

7.2 Ancient megafauna sediment data. Sequences were filtered and sorted using the programs included in the OBITools package (http://metabarcoding.org/obitools). For filtering, only reads containing both primers and the tag were kept in the data, permitting two errors in the primers and no errors in the tags. Filtering and taxonomic identification was performed as described in ref. 57 with the following two adjustments: (1) an additional denoising step using the program Obiclean was included[89]; and (2) the electronic PCR was performed on the EMBL standard sequences release 111. Within each sample, only sequences represented by >10 reads and an identification to at least genus level with an identity >0.95 were kept in the final data set. Identified taxa in each of the samples for which plant data are available are given in Extended Data Table 5.

7.3 Ancient megafauna diet data. The plant DNA amplified from coprolites and intestinal/stomach content was sorted using the OBITools package (http://metabarcoding.org/obitools). Sequences shorter than 10 bp, or containing ambiguous nucleotides, or with occurrence ≤5 were excluded. Strictly identical sequences were merged and taxonomic assignation was achieved using the ecoTag program and reference libraries described in sections 5.1 and 5.2. Only unique sequences with an identity of 100% to at least one of the reference sequences were kept for further analysis. Where 100% identities were obtained from multiple reference libraries, priority was given to taxon assignment using the Arctic and boreal libraries.

We obtained a total of 15,951 sequence reads that could be assigned to the eight coprolite/gut samples using the MID tags, of which 1,663 reads were unique. Out of these reads, 13,735 passed filtering and a final 9,084 reads could be assigned with 100% identity to a plant species in one of the reference databases. Sequence data and compositional data for the fossil diet samples are given in Supplementary Data 6.

8.1 Published permafrost sites, Eurasia. Bol'shaya Balakhnaya, Buor Khaya and Khatanga, northwest Siberia: three locations in northwest Siberia with perennially frozen deposits are described in ref. 16. Buor Khaya is located on the east side of the bay formed by the Lena Delta; is a 3-m exposure of sandy silt with organic inclusions, interpreted as lacustrine sediment, Holocene in age. Khatanga material was sampled from Holocene river terrace deposits (<5 m) along a small tributary stream. Material ranged from clay, to weakly laminated sands and silts, to peat. Bol'shaya Balakhnaya is also a Holocene fluvial terrace locality featuring weakly laminated sands and minor interspersed lenses of peat and clay.

Baskura Peninsula, Cape Sabler, Federov Island, Ovrazhny Peninsula, and Upper Taymyr River, Taimyr Peninsula, northwest Siberia: these localities are described in ref. 7, which reports perennially frozen sediments taken along the shore of Taimyr Lake. Deposits are silt-dominated but range from organic to inorganic, and massive to laminated; all sediments are of Late Pleistocene age (~40–12 kyr). Further stratigraphic information from the 'type locality' of this type of sediment—Cape Sabler—is provided in ref. 90. Sediment depth/age curves in ref. 7 show that depositional rates were in the order of 1–2 mm yr^{-1}. This implies a high temporal resolution of the trapped macroflora elements and other biogenic matter, as the ground surface rose due to the vertical accretion of silt and fine sand that was transported and deposited by aeolian and surface runoff processes.

Main River, east Siberia: the Main River (Ice Bluff) exposure extends for about 1 km on the left bank of the Main River. It has been previously reported in refs 90 and 91. The northern exposure, from where our samples are derived, is dominated by ice-rich deposits interpreted as a facies of yedoma in ref. 92. At the time of sampling, the lower portion of the exposure was covered by slump material; the oldest exposed deposits are ~40 kyr. We dated further samples to improve the previously established chronology of the site (Extended Data Fig. 1a). Samples form a consistent progression suggesting continuous sedimentation without major hiatus between ~40 and 20 kyr.

8.2 Unpublished permafrost sites, Eurasia. Taimyr Lake, Taimyr Peninsula, northwest Siberia: a 3-m high cliff section on the western side of the Cape Sabler Peninsula. Vaguely laminated silt with some sand intrabeds. Four radiocarbon dates suggest a mid-Holocene age between 4.7–7.1 kyr for the sediment sequence, except for the uppermost sample that is modern in age.

Anadyr, east Siberia: Holocene deposits, beside the Anadyr River, 2 km west of Anadyr, Chukotka. Materials excavated from a pit lying 3.0–5.1 m above sea level.

Duvanny Yar, northeast Siberia: the site is the type section for the Late Pleistocene in northeast Siberia and has been much studied (for example, refs 93–95). The extensive set of exposures runs for ~4 km along the east bank of the Kolyma River and features high cliffs of yedoma (ice complex), dominated by silt and large syngenetic ice wedges, depressions representing the drained basins of thermokarst lakes (alasy), and large areas of slumped and partially vegetated material. The exposure we studied and sampled in 2009 (Extended Data Fig. 1b) underlies the same remnant yedoma surface as identified by ref. 93. We levelled in and logged 23 sections and sampled for DNA, radiocarbon and palaeoecological analysis from just above the Kolyma River level to ~40 m above it.

The sampled stratigraphic unit comprised yedoma sandy silt at least 34 m thick, underlying a thaw unconformity at a depth of ~1.9 m below the ground surface (Extended Data Fig. 1c). The yedoma unit was characterized by grey sandy silt to silty fine sand with low and varying amounts of organic matter, the most prominent of which were abundant fine *in situ* roots pervasive throughout the unit. The

sediment is interpreted primarily as loess and contains a number of weakly developed palaeosols (J.B. Murton, unpublished data). The upper 1.9 m of the sedimentary sequence comprised the postglacial transition zone and overlying modern active layer.

A ^{14}C age-depth model is presented in Extended Data Fig. 1d. The upper part of the model, above an elevation of 20 m above river level, is considered to be robust, based on ^{14}C ages that decrease overall in stratigraphic order towards the top of the unit. ^{14}C ages from below 15–20 m above river level are close to the limit of radiocarbon dating, and the age-depth model of this lower part of the yedoma should be treated as less definitive, although supported by OSL (optically stimulated luminescence) age at 14.5 m. The basal units of the exposure are not represented in this study.

Svalbard: Colesdalen and Endalen: samples were taken from the upper organic horizon of tundra soils in two valleys directly into sterile tubes and sealed. Sites are Colesdalen and Endalen (Extended Data Fig. 1e, f). Both valleys have vegetation dominated by mid-Arctic tundra.

8.3 Published permafrost sites, North America. Zagoskin Lake, Alaska: Zagoskin is a maar lake in western Alaska with sediments dating from ~37 kyr BP. Details are reported in refs 96, 97. The sediments are relatively inorganic and dominated by silt, interpreted as loess[97]. Loss on ignition values are generally <10%, except in the top 1.4 m of the 15-m section. Biostratigraphic changes related to deglaciation (~15 kyr BP) are recorded at 5 m depth. Sediments dating to the LGM are present.

Quartz Creek, Yukon Territory, Canada: This locality is described in ref. 98. Sections are exposed in mining cuts and comprise silt-rich facies and palaeosols. The silt is loess-derived and sometimes finely bedded, reflecting re-working. Samples are associated with the Late Pleistocene Dawson tephra[98,99] and immediately underlie the bed, ranging from 31 to 30 kyr BP, consistent with the Dawson tephra chronology.

Goldbottom, Yukon Territory, Canada: This locality also comprises several exposures in mining cuts and is described in ref. 100. Frozen silt-dominated sediments, interpreted as loess or re-transported loess, and organic deposits are present, and the Dawson tephra provides a late MIS 3–early MIS 2 stratigraphic marker. Previous dating of the tephra at ca. 30 kyr BP[100,101] are consistent with ages associated with the samples in this study. Samples at the site range include pre-LGM samples (ca. 45–27 kyr BP) and early LGM ages (ca. 24–23 kyr BP).

Stevens Village, Alaska: The locality is described in ref. 6. The exposure is ~15 m high and lies on the Yukon River in central Alaska. Frozen silt, interpreted as loess, overlies basal fluvial gravel and contains interbedded organic layers (regosols) dating to the early Holocene. A single sample collected from an early Holocene soil dates to 11.2 kyr BP.

8.4 Unpublished permafrost sites, North America. Purgatory, Alaska: The Purgatory site is located a few kilometres upstream from the Stevens Village site and consists of aeolian sands with plant detritus. Two samples from near the base of the exposure date to the post-LGM interval.

Ross Mine, Canada: the Ross Mine site is located in the southern Klondike goldfields of central Yukon. One sample from a floodplain silt unit within fluvial deposits dates to the LGM, whereas the remaining samples, collected from within a Holocene peatland, date to the post-LGM interval.

51. Willerslev, E. *et al.* Ancient biomolecules from deep ice cores reveal a forested southern Greenland. *Science* **317,** 111–114 (2007).
52. Epp, L. S. *et al.* New environmental metabarcodes for analysing soil DNA: potential for studying past and present ecosystems. *Mol. Ecol.* **21,** 1821–1833 (2012).
53. Vestergård, M. Nematode assemblages in the rhizosphere of spring barley (*Hordeum vulgare* L.) depended on fertilisation and plant growth phase. *Pedobiologia* **48,** 257–265 (2004).
54. Brock, F., Higham, T., Ditchfield, P. & Ramsey, C. B. Current pretreatment methods for AMS radiocarbon dating at the Oxford Radiocarbon Accelerator Unit (ORAU). *Radiocarbon* **52,** 103–112 (2010).
55. Hua, Q. & Barbetti, M. Review of tropospheric bomb 14C data for carbon cycle modeling and age calibration purposes. *Radiocarbon* **46,** 1273–1298 (2007).
56. Goslar, T., Van der Knaap, W. O., Kamenik, C. & van Leeuwen, J. Free-shape 14C age–depth modelling of an intensively dated modern peat profile. *J. Quaternary Sci.* **24,** 481–499 (2009).
57. Boessenkool, S. *et al.* Blocking human contaminant DNA during PCR allows amplification of rare mammal species from sedimentary ancient DNA. *Mol. Ecol.* **21,** 1806–1815 (2012).
58. Haile, J. in *Methods in Molecular Biology – Ancient DNA* (eds Shaprio, B. & Hofreiter, M.) 57–63 (Humana Press Series, 2012).
59. Coissac, E. OligoTag: a program for designing sets of tags for next-generation sequencing of multiplexed samples. *Methods Mol. Biol.* **888,** 13–31 (2012).
60. Ait Baamrane, M. A. *et al.* Assessment of the food habits of the Moroccan dorcas gazelle in M'Sabih Talaa, west central Morocco, using the *trn*L approach. *PLoS ONE* **7,** e35643 (2012).
61. Taylor, P. G. Reproducibility of ancient DNA sequences from extinct Pleistocene fauna. *Mol. Biol. Evol.* **13,** 283–285 (1996).
62. Binladen, J. *et al.* The use of coded PCR primers enables high-throughput sequencing of multiple homolog amplification products by 454 parallel sequencing. *PLoS ONE* **2,** e197 (2007).
63. Jackson, S. T. Representation of flora and vegetation in Quaternary fossil assemblages: known and unknown knowns and unknowns. *Quat. Sci. Rev.* **49,** 1–15 (2012).
64. Birks, H. J. B. & Birks, H. H. *Quaternary Palaeoecology* (London Edward Arnold, 2004).
65. Höfle, C. & Ping, C.-L. Properties and soil development of late-Pleistocene paleosols from Seward Peninsula, northwest Alaska. *Geoderma* **71,** 219–243 (1996).
66. Tomašových, A. & Kidwell, S. M. Predicting the effects of increasing temporal scale on species composition, diversity, and rank-abundance distributions. *Paleobiology* **36,** 672–695 (2010).
67. Cornelissen, J. H. C. *et al.* Global negative vegetation feedback to climate warming responses of leaf litter decomposition rates in cold biomes. *Ecol. Lett.* **10,** 619–627 (2007).
68. Aerts, R. & Chapin, F. S. I. The mineral nutrition of wild plants revisited: a re-evaluation of processes and patterns. *Adv. Ecol. Res.* **30,** 1–67 (1999).
69. Crooks, G. E., Hon, G., Chandonia, J.-M. & Brenner, S. E. WebLogo: a sequence logo generator. *Genome Res.* **14,** 1188–1190 (2004).
70. Dansgaard, W. *et al.* Evidence for general instability of past climate from a 250-kyr ice-core record. *Nature* **364,** 218–220 (1993).
71. Oksanen, J. Multivariate analysis of ecological communities in R: vegan tutorial. *R package version 1.17-7* (2011).
72. Caliński, T. & Harabasz, J. A dendrite method for cluster analysis. *Commun. Stat.* **3,** 1–27 (1974).
73. Kühn, I., Durka, W. & Klotz, S. BiolFlor — a new plant-trait database as a tool for plant invasion ecology. *Divers. Distrib.* **10,** 363–365 (2004).
74. McCune, B., Grace, J. B. & Urban, D. L. Analysis of ecological communities. MjM Software, Gleneden Beach, Oregon, USA (http://www.pcord.com) (2002).
75. Clarke, K. R., Somerfield, P. J. & Chapman, M. G. On resemblance measures for ecological studies, including taxonomic dissimilarities and a zero-adjusted Bray–Curtis coefficient for denuded assemblages. *J. Exp. Mar. Biol. Ecol.* **330,** 55–80 (2006).
76. Austin, M. P. Inconsistencies between theory and methodology: a recurrent problem in ordination studies. *J. Veg. Sci.* **24,** 251–268 (2013).
77. Faith, D. P., Minchin, P. R. & Belbin, L. Compositional dissimilarity as a robust measure of ecological distance. *Vegetatio* **69,** 57–68 (1987).
78. Legendre, P. & Legendre, L. *Numerical Ecology* (Elsevier, 1998).
79. Anderson, M. J., Connell, S. D. & Gillanders, B. M. Relationships between taxonomic resolution and spatial scales of multivariate variation. *J. Anim. Ecol.* **74,** 636–646 (2005).
80. Gotelli, N. J. & Colwell, R. K. in *Biological Diversity: Frontiers in Measurement and Assessment* (Magurran, A. E. & McGill, B. J.) 39–54 (Oxford Univ. Press, 2011).
81. Walther, B. A. & Moore, J. L. The concepts of bias, precision and accuracy, and their use in testing the performance of species richness estimators, with a literature review of estimator performance. *Ecography* **28,** 815–829 (2005).
82. Hortal, J., Borges, P. A. V. & Gaspar, C. Evaluating the performance of species richness estimators: sensitivity to sample grain size. *J. Anim. Ecol.* **75,** 274–287 (2006).
83. Vavrek, M. J. Fossil: palaeoecological and palaeogeographical analysis tools. *Palaeontol. Electronica* **14** (1T), 16p (2011).
84. Dunn, P. K. Tweedie: tweedie exponential family models. *R package version 2.1.7* (2011).
85. Davison, J., Öpik, M. & Daniell, T. J. Arbuscular mycorrhizal fungal communities in plant roots are not random assemblages. *FEMS Microbiol. Ecol.* **78,** 103–115 (2011).
86. Munch, K., Boomsma, W., Huelsenbeck, J. P., Willerslev, E. & Nielsen, R. Statistical assignment of DNA sequences using Bayesian phylogenetics. *Syst. Biol.* **57,** 750–757 (2008).
87. Roberts, D. W. labdsv: ordination and multivariate analysis for ecology. *R package version 1.5-0* (2007).
88. Underwood, A. J. *Experiments in Ecology: Their Logical Design and Interpretation Using Analysis of Variance* (Cambridge Univ. Press, 1997).
89. Shehzad, W. *et al.* Prey preference of snow leopard (*Panthera uncia*) in South Gobi, Mongolia. *PLoS ONE* **7,** e32104 (2012).
90. Möller, P., Bolshiyanov, D. Y. & Bergsten, H. Weichselian geology and palaeoenvironmental history of the central Taymyr Peninsula, Siberia, indicating no glaciation during the last global glacial maximum. *Boreas* **28,** 92–114 (1999).
91. Kuzmina, S. A. *et al.* The late Pleistocene environment of the Eastern West Beringia based on the principal section at the Main River, Chukotka. *Quat. Sci. Rev.* **30,** 2091–2106 (2011).
92. Kotov, A. N., Lozhkin, A. V. & Ryabchun, V. K. in *Formation of Relief, Correlated Sediments and Placer Deposits of the Northern-East of the USSR, SVKNII DVO AN USSR, Magadan* 117–131 (1989).
93. Sher, A. V. *et al.* Late Cenozoic of the Kolyma Lowland. *XIV Pacific Science Congress, Khabarovsk* 1–116 1979).
94. Wetterich, S., Schirrmeister, L. & Kholodov, A. L. The joint Russian-German expedition Beringia/Kolyma 2008 during the International Polar Year (IPY) 2007/2008. *Reports on Polar and Marine Research* **636,** 43 (2011).
95. Zanina, O. G., Gubin, S. V. & Kuzmina, S. A. Late-Pleistocene (MIS 3-2) palaeoenvironments as recorded by sediments, palaeosols, and ground-squirrel nests at Duvanny Yar, Kolyma lowland, northeast Siberia. *Quat. Sci. Rev.* **30,** 2107–2123 (2011).
96. Ager, T. A. Late Quaternary vegetation and climate history of the central Bering land bridge from St. Michael Island, western Alaska. *Quat. Res.* **60,** 19–32 (2003).
97. Muhs, D. R., Ager, T. A., Been, J., Bradbury, J. P. & Dean, W. E. A late Quaternary record of eolian silt deposition in a maar lake, St. Michael Island, western Alaska. *Quat. Res.* **60,** 110–122 (2003).

98. Sanborn, P. T., Smith, C. A., Froese, D. G. & Zazula, G. D. Full-glacial paleosols in perennially frozen loess sequences, Klondike goldfields, Yukon Territory, Canada. *Quat. Res.* **66,** 147–157 (2006).
99. Zazula, G. D., Froese, D. G., Elias, S. A. & Kuzmina, S. Arctic ground squirrels of the mammoth-steppe: paleoecology of Late Pleistocene middens (~24000–29450 ^{14}C yr BP), Yukon Territory, Canada. *Quat. Sci. Rev.* **26,** 979–1003 (2007).
100. Froese, D. G., Zazula, G. D. & Reyes, A. V. Seasonality of the late Pleistocene Dawson tephra and exceptional preservation of a buried riparian surface in central Yukon Territory, Canada. *Quat. Sci. Rev.* **25,** 1542–1551 (2006).
101. Demuro, M. *et al.* Optically stimulated luminescence dating of single and multiple grains of quartz from perennially frozen loess in western Yukon Territory, Canada: comparison with radiocarbon chronologies for the late Pleistocene Dawson tephra. *Quat. Geochronol.* **3,** 346–364 (2008).
102. Beilman, D. W. Holocene and recent carbon accumulation in Svalbard mires. Svalbard Geology Workshop, Tromso Norway 27–29 April (2011).
103. Kosintsev, P. A. *et al.* Environmental reconstruction inferred from the intestinal contents of the Yamal baby mammoth Lyuba (*Mammuthus primigenius* Blumenbach, 1799). *Quat. Int.* **255,** 231–238 (2012).
104. Boeskorov, G. G. *et al.* Woolly rhino discovery in the lower Kolyma River. *Quat. Sci. Rev.* **30,** 2262–2272 (2011).
105. Harington, C. R. & Eggleston-Stott, M. Partial carcass of a small Pleistocene horse from Last Chance Creek near Dawson City, Yukon. *Curr. Res. Pleistocene* **13,** 105–107 (1996).
106. Sulerzhitsky, L. D. & Romanenko, F. A. Age and dispersal of 'mammoth' fauna in Asian Polar region (according to radiocarbon data). *Kriosfera Zemli* **1,** 12–19 (1997).
107. Lazarev, P. A. in: *Mammals of the Yakutian Anthropogene* (ed, Labutin, Y.) 55–97 [in Russian] (Russian Acad. Sci. 1998).
108. Kosintsev, P. A., Lapteva, E. G., Korona, O. M. & Zanina, O. G. Living environments and diet of the Mongochen mammoth, Gydan Peninsula, Russia. *Quat. Int.* **276–277,** 253–268 (2012).

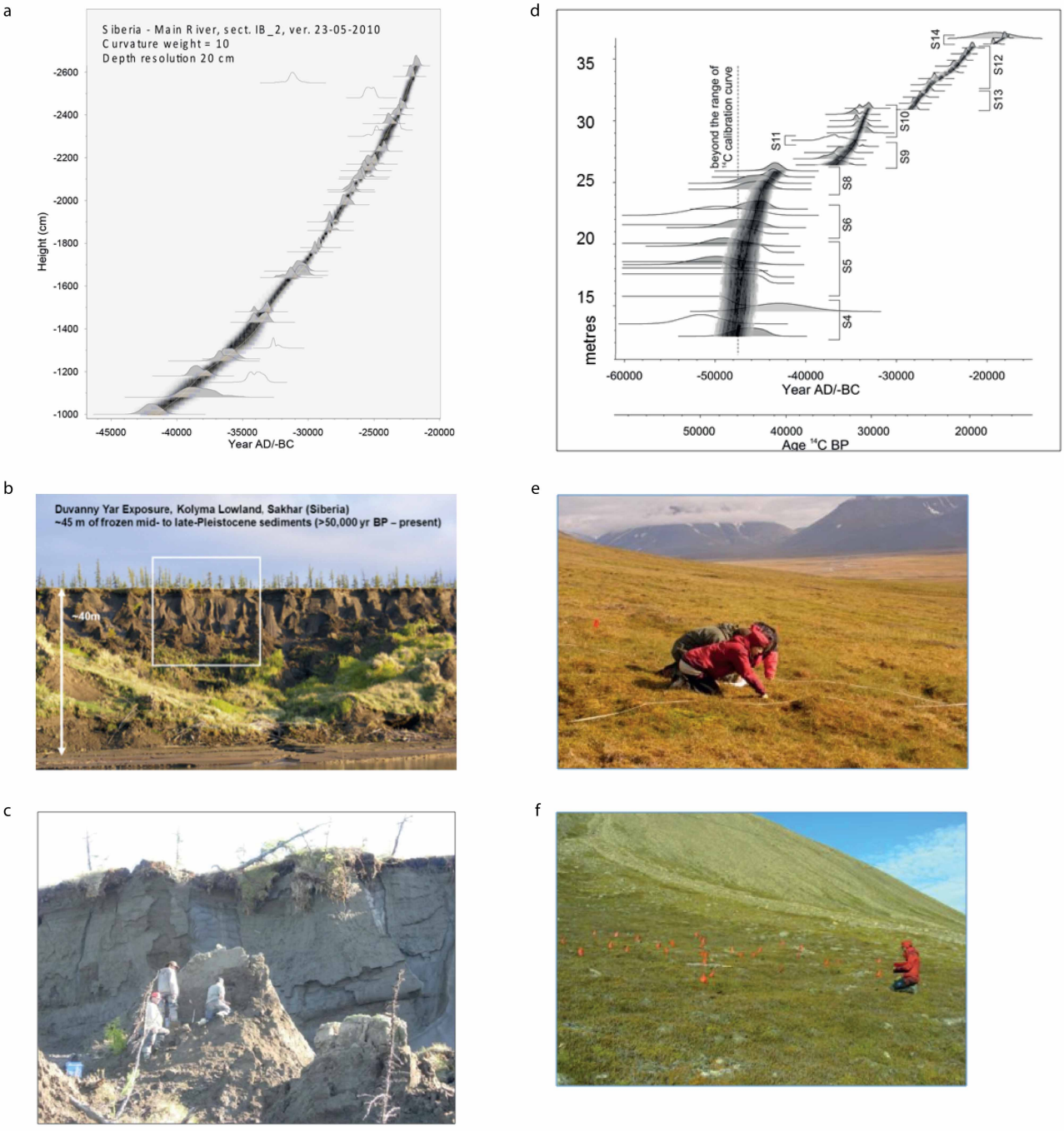

Extended Data Figure 1 | Permafrost sample locality details. **a**, Radiocarbon dating chronology for the main section at the Main River site, Russia, from which nearly all Main River samples are derived. **b**, View of the 2009 Duvanny Yar exposure, northeast Siberia. **c**, yedoma sandy silt in upper c. 12 m of the exposure at Duvanny Yar exposure, northeast Siberia. A large syngenetic ice wedge (top centre) within the yedoma is truncated by a thaw unconformity at a depth of c. 1.9 m below the ground surface, marking the maximum postglacial thaw depth after deposition of the yedoma had ended. People shown for scale, with DNA sediment sample holes to the right of the person on right. **d**, Calibrated radiocarbon date distributions plotted against depth above river level at Duvanny Yar exposure, northeast Siberia. Although there are some finite dates below ~20 m, the general curve shape suggests the radiocarbon dating limit occurs at about this level. **e**, **f**, The two Svalbard sites at Colesdalen (**e**) and Endalen (**f**).

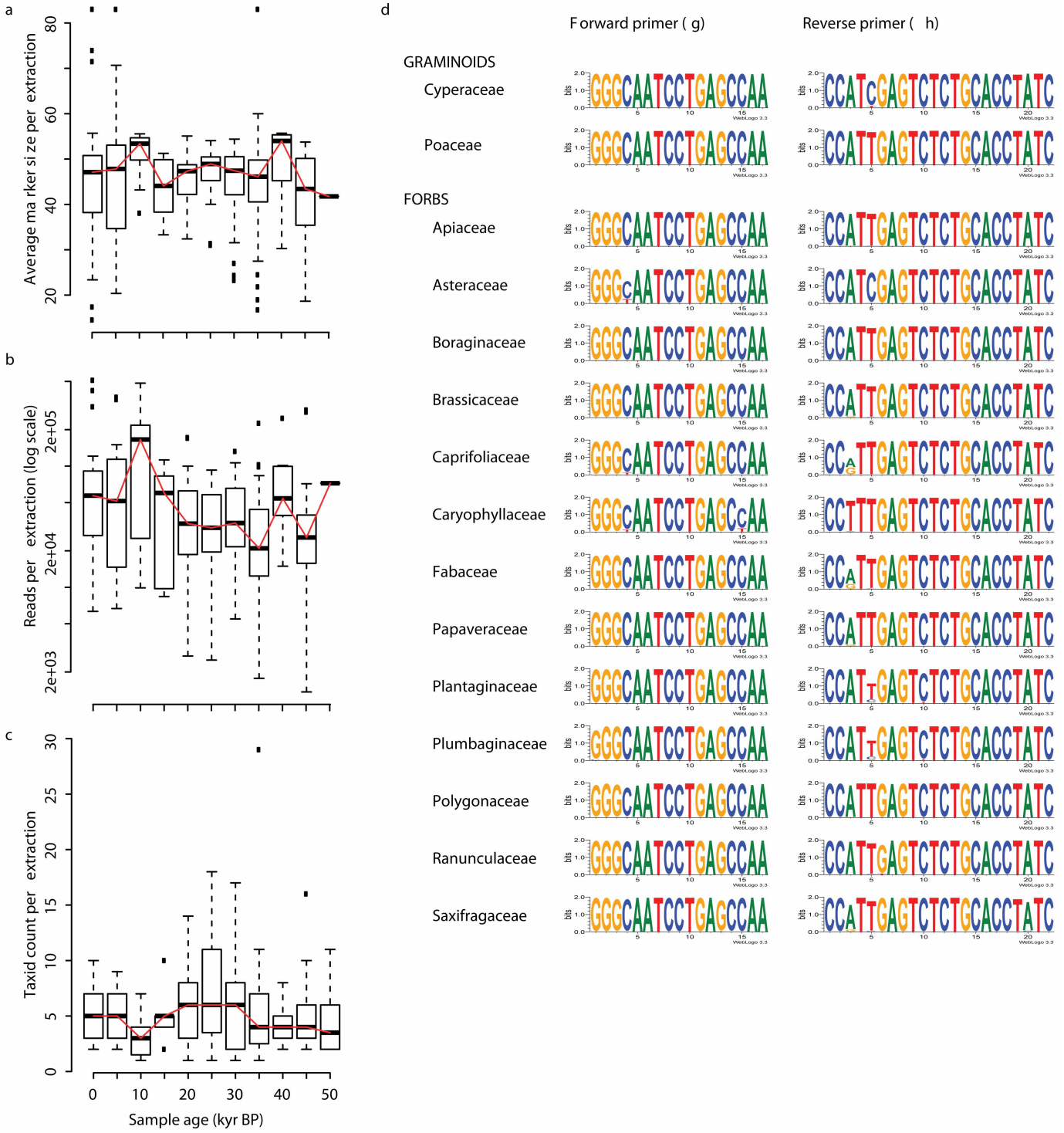

Extended Data Figure 2 | MOTU characterization and data consistency. **a**–**c**, Graphs showing the consistency of the DNA-based approach using permafrost samples across the different time periods: average marker size per sample (**a**); number of reads per sample (**b**); number of taxa per sample (**c**). **d**, WebLogos showing the match between the *gh* primers and their target sequences in the main plant families involved in the estimation of the proportions of forbs and graminoids[70].

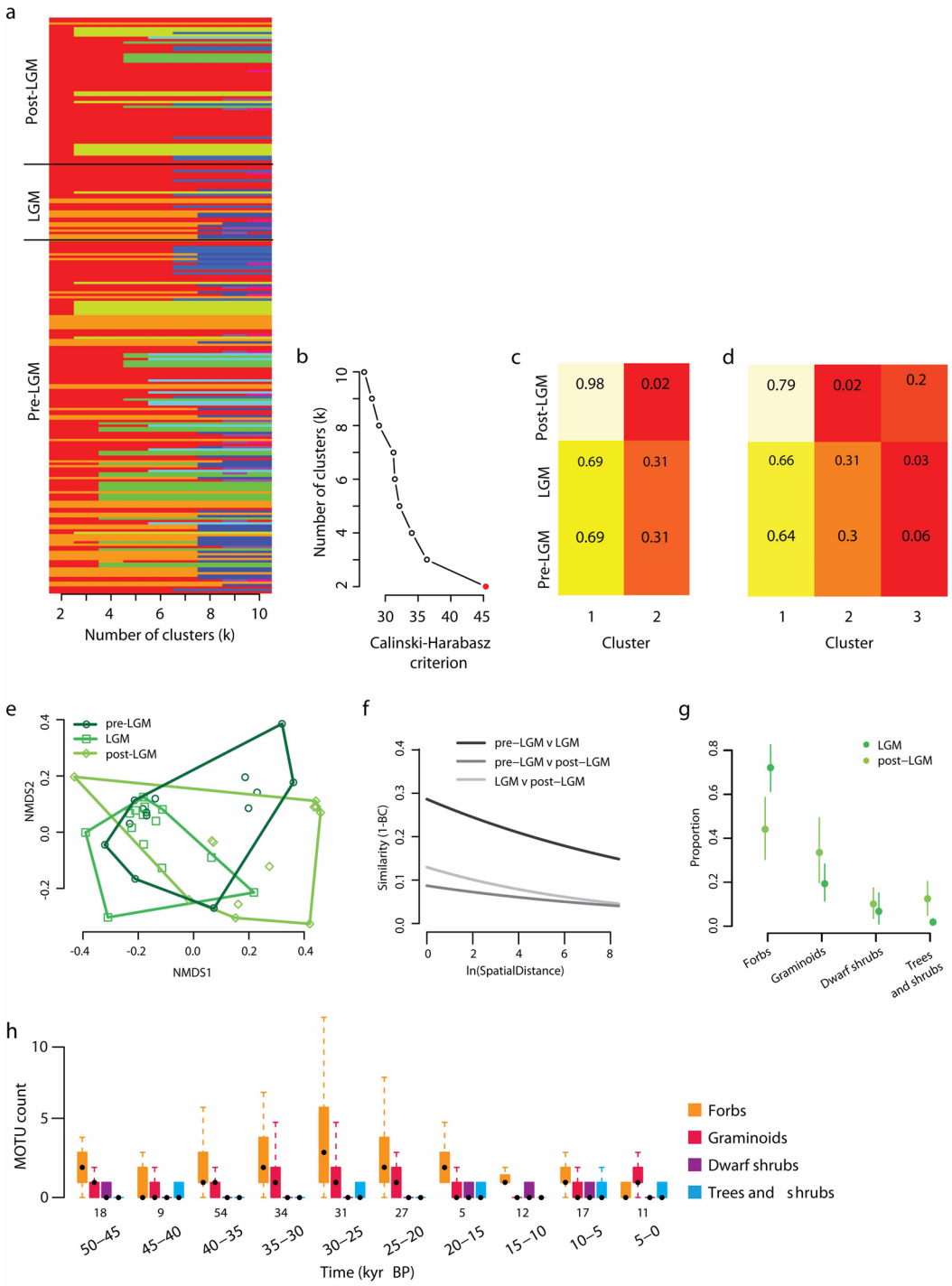

Extended Data Figure 3 | Temporal classification of samples, assemblage variation in time and data robustness. **a**–**d**, *K*-means clustering of permafrost plant assemblages. **a**, Cluster identity of samples derived from pre-LGM, LGM and post-LGM periods for values of *K* between 2 and 10. Each bar represents a separate sample; different colours reflect different cluster identities. **b**, The Calinski–Harabasz criterion for different levels of *K*. Higher values indicate stronger support for a level of partitioning. **c**, **d**, Heat maps showing the proportional occurrence of samples from pre-LGM, LGM and post-LGM periods in different clusters, for $K = 2$ (**c**) and $K = 3$ (**d**). Colours vary from red (low values) to white (high values). **e**–**g**, Assemblage variation in time and space. **e**, Nonmetric multidimensional scaling (NMDS) ordination revealed significant variation (PERMANOVA, $P < 0.01$) in fossil/ancient plant assemblage composition during the three palaeoclimatic periods. **f**, The effect of spatial distance on similarity when assemblages from different palaeoclimatic periods were compared. The vertical axis represents similarity in floristic composition measured as 1-Bray–Curtis similarity, the horizontal axis depicts ln of distance between sampled communities in kilometres. The greater the spatial distance between pairs of assemblages, the more dissimilar they were. However, the rate of the decay differed depending on which two climatic periods were compared (full model $P < 0.001$). The weakest distance decay in similarity was observed in the case of comparisons between pre-LGM and post-LGM assemblages. Even if pre-LGM and post-LGM samples came from the same geographic area, their floristic compositions were dissimilar. **g**, Results of randomization tests. Mean proportional composition of different growth form types in LGM and post-LGM samples. The bars around sample means indicate 95% quantiles derived from 999 bootstrap replicates (where bootstrap *N* was set to the number of samples in the post-LGM data set; see methods for details). **h**, Counts of MOTUs exhibiting different growth forms binned over 5-kyr time intervals. The analysis included 218 of the 242 sediment samples, as described in Fig. 4. Numbers immediately below the columns indicate sample sizes. Median (central dot), quartile (box), maximum and minimum (whiskers) counts are shown.

Extended Data Table 1 | Site information of the 21 permafrost localities (shown in Fig. 1)

Site	LAT	LON	Sample size			Sediment type	Source of stratigraphic description
			pre-LGM	LGM	post-LGM		
Anadyr, Russia	64.74	177.31	0	0	3	Holocene peat	Ecochange, unpublished
Baskura Peninsula, Russia	74.66	101.28	10	3	0	Silts and fine sand of the "ice complex"	7
Bol'shaya Balaknaya, Russia	73.65	102.12	6	2	4	unconformable fluvial units	16
Buor Kaya, Russia	71.91	132.79	0	0	7	Holocene thermokarst lake sediments	16
Cape Sabler, Russia	74.55	100.54	9	0	0	Silts and fine sand of the "ice complex"	90 ; 7
Colesdalen, Svalbard	78.04	15.12	0	0	3	Soil underlying modern vegetation	Ecochange, unpublished
DuvannyYar, Russia	68.67	159.08	71	6	4	Silts and fine sand of the "ice complex"	Ecochange, unpublished but see other studies, for example 103; 96
Endalen, Svalbard	78.13	15.72	0	0	8	Soil underlying modern vegetation	Soil sample under modern vegetation, Ecochange unpublished
Federov Island, Russia	74.62	100.71	0	0	6	Silts and fine sand of the "ice complex"	7
Goldbottom, Canada	63.93	221.03	8	3	0	Silt (loess and related deposits)	100
Khatanga, Russia	71.99	102.24	0	0	3	Silt-dominated fluvial terrace	16
Main River, Russia	64.28	171.25	28	15	0	Silt (loess and related deposits)	91
Ovrazhny Peninsula, Russia	75.15	100.12	5	0	0	Silts and fine sand of the "ice complex"	7
Purgatory, Alaska	66.23	211.73	0	0	2	Interbedded loess/paleosols	D. Froese, unpublished
Quartz Creek, Canada	63.82	220.97	7	0	0	Silt (loess and related deposits)	D. Froese, unpublished
Ross Mine, Canada	63.69	221.42	0	1	4	Silt (loess and related deposits)	D. Froese, unpublished
Stevens Village, Alaska	65.98	211.05	0	0	1	Interbedded loess/palaeosols	6
Stuphallet, Svalbard	78.96	11.60	0	0	10	Holocene peat	102
Taimyr Lake, Russia	74.53	100.50	0	0	5	Bedded silt (Holocene)	Ecochange, unpublished
Upper Taymyr River, Russia	74.27	99.83	4	2	0	Silts and fine sand of the "ice complex"	7
Zagoskin Lake, Alaska	63.47	197.95	1	0	1	Lacustrine sediment	96

Extended Data Table 2 | Statistics regarding length of the P6 loop amplified with the *gh* primers[41] for the most important plant families of the two growth forms (graminoids and forbs)

Growth form	Family	Minimum (bp)	Maximum (bp)	Mean (bp)	Standard deviation (bp)	Number of sequence variants	Total number of sequences
Graminoids	Cyperaceae	77	122	88.3	12.0	82	235
	Poaceae	39	59	53.0	3.7	63	258
Forbs	Apiaceae	40	57	46.0	3.6	26	57
	Asteraceae	46	55	50.1	1.5	44	234
	Boraginaceae	33	47	42.4	4.4	9	18
	Brassicaceae	38	53	47.6	2.4	53	128
	Caprifoliaceae	46	58	49.5	3.3	12	19
	Caryophyllaceae	22	66	49.8	11.6	64	127
	Fabaceae	24	65	54.9	6.8	36	73
	Papaveraceae	51	54	53.0	1.4	4	24
	Plantaginaceae	39	52	43.6	3.5	28	39
	Plumbaginaceae	23	23	23.0	0.0	1	1
	Polygonaceae	27	32	30.6	1.7	16	50
	Ranunculaceae	27	72	52.8	7.3	62	116
	Saxifragaceae	22	58	42.7	14.3	34	56

These data were estimated from the Arctic/boreal database built for this study.

Extended Data Table 3 | Locality information of the seven contemporary tundra and steppe sites in Yukon, Canada, which were analysed for nematode faunal composition (shown in Fig. 3)

Locality	Coordinates and elevation ASl (m)	Site description
Blackstone River (a)	64°50'N, 138°19'W; 998 m	Shrub tundra with *Salix* and *Betula*, graminoid tussocks, *Eriophorum*, *Rhododendron* subsect. Ledum (Labrador tea), *Vaccinium vitis idaea* (lingon berry), *Rubus chamaemorus*, mosses and lichens.
Ogilvie Mountains (b)	65°04'N, 138°15'W; 1043 m	Tussock tundra with *Eriophorum*, *Rhododendron* subsect. Ledum, *Rubus chamaemorus*, *Arctostaphylos*, shrub *Salix* and *Betula* and mosses.
Eagle Plains South (c)	65°51'N, 137°41'W; 860 m	*Betula* and *Salix* shrubs with *Rhododendron* subsect. Ledum, *Vaccinium vitis idaea*, *Rubus chamaemorus*, *Arctostaphylos*, *Empetrum nigrum*, graminoids, mosses and lichens.
Eagle Plains North (d)	66°30'N, 136°31'W; 724 m	Tussock tundra with *Eriophorum*, *Rhododendron* subsect. Ledum, *Rubus chamaemorus*, *Empetrum nigrum*, shrub *Alnus*, *Betula* and *Salix* as well as mosses and lichens.
Little Atlin Lake (e)	60°17'N, 133°58'W; 719 m	Grasses, lichens, *Linum*, *Artemisia frigida*, *Astragulus*, *Potentilla*, *Anemone pulsatilla* and other forbs
Kluane Lake (f)	61°09'N, 138°24' W; 828 m	S-facing slope, graminoids, lichens, *Artemisia frigida*, *Anemone pulsatilla ludoviciana* and other forbs.
Carmacks (g)	62°05'N, 136°19'W; 605 m	SW-facing slope with tall and short grasses, *Artemisia frigida, Bupleurum, Anemone pulsatilla* and lichens.

Letters in parentheses refer to locality codes used in Figs 1 and 3.

Extended Data Table 4 | Proportion of 17 permafrost sediments with sequences of the two indicator nematode families Cephalobidae and Teratocephalidae

Age range of sediment samples (yr BP)	Cephalobidae	Teratocephalidae
9,403-6,745	1.00	0.50
39,174-12,567	0.92	0.08

Extended Data Table 5 | Herbivorous mammal taxa derived from Main River permafrost samples for which plant data were available

Site	Region	ID number	Taxa
Main River	Siberia	EH0293	*Mammuthus primigenius, Alces alces*
Main River	Siberia	EH0294	*Mammuthus primigenius, Equus caballus*
Main River	Siberia	EH0345	*Mammuthus primigenius*
Main River	Siberia	EH0341	
Main River	Siberia	EH0339	
Main River	Siberia	EH0338	*Mammuthus primigenius*
Main River	Siberia	EH0279	*Mammuthus primigenius*
Main River	Siberia	EH0280	*Mammuthus primigenius*
Main River	Siberia	EH0320	*Coelodonta antiquitatis*
Main River	Siberia	EH0315	*Mammuthus primigenius, Lepus*
Main River	Siberia	EH0311	*Mammuthus primigenius*
Main River	Siberia	EH0310	*Mammuthus primigenius*
Main River	Siberia	EH1027	
Main River	Siberia	EH0295	*Mammuthus primigenius, Alces alces*
Main River	Siberia	EH0296	
Main River	Siberia	EH0282	*Mammuthus primigenius, Rangifer tarandus, Alces alces*
Main River	Siberia	EH0343	*Alces alces*
Main River	Siberia	EH0344	*Alces alces*
Main River	Siberia	EH0300	*Mammuthus primigenius*
Main River	Siberia	EH0994	
Main River	Siberia	EH0317	*Mammuthus primigenius*
Main River	Siberia	SL042	
Main River	Siberia	EH1026	*Mammuthus primigenius*
Main River	Siberia	EH0995	*Mammuthus primigenius*
Main River	Siberia	EH0075	

Extended Data Table 6 | Sample information of the eight megafauna gut and coprolite samples from woolly mammoth (*Mammuthus primigenius*), bison (*Bison sp.*), woolly rhinoceros (*Coelodonta antiquitatis*) and horse (*Equus lambei*) (shown in Fig. 1)

Species	Name	Reference	Material	14C age of sample	Calendar age (95.4%)		14C lab ID	Locality Fig. 1	Location of Discovery	Coordinates	DNA lab ID
Woolly mammoth	Drevniy Creek Mammoth	This publication	Coprolite	>52,000	Infinite		Poz-37540	A	NE Yakutia	68°35'N, 161°45'E	12
Bison	Bison	This publication	Coprolite	>52,000	Infinite		Poz-37542	B	NE Yakutia	68°44'N, 161°38'E	13
Woolly mammoth	Lyuba Mammoth	103	Intestine	41,700 ± 625	46,150	44,320	GrA-41861	C	Yamal Peninsula	68°38'N, 71°40'E	2
Woolly rhinoceros	Kolyma Rhino	104	Stomach	39,140 ± 390	44,120	42,706	OxA-18755	D	NE Yakutia	68°46'N, 161°38'E	10
Horse	Last Chance Creek Horse	105	Gut	26,280 ± 210	31,225	30,560	Beta-67407	E	Last Chance Creek near Dawson City, Yukon	65°32'N, 164°29'W	22
Woolly rhinoceros	Churapcha Rhino	106, 107	Gut	19,500 ± 120	23,686	22,667	GIN-9594	F	Central Yakutia, Churapcha settlement	62°0'N, 132°25'E	1
Woolly mammoth	Mongochen Mammoth	108	Colon	18,370 ± 150	22,316	21,496	LE-8664	G	Gydan Peninsula	72°10'N, 79°35'E	3
Woolly mammoth	Finish Creek Valley Mammoth	This publication	Coprolite	17,980 ± 90	21,819	21,141	Poz-37541	H	NE Yakutia	68°43'N, 161°35'E	11